



A novel approach to include small reservoirs into a global hydrological model: Assessing its potential to reduce the agricultural water gap of smallholder farmers in Senegal

Anna C. Hoogeveen^{a,b}, Edwin H. Sutanudjaja^a, Gatien N. Falconnier^{c,d,e,f}, L.P.H. (Rens) van Beek^a, Niko Wanders^a, Marc F.P. Bierkens^{a,g}, Jannis M. Hoch^{a,h,*}

^a Department of Physical Geography, Utrecht University, Utrecht, the Netherlands

^b Tauw, Deventer, the Netherlands

^c AIDA, University of Montpellier, CIRAD, Montpellier, France

^d CIRAD, UPR AIDA, Harare, Zimbabwe

^e International Maize and Wheat Improvement Centre (CIMMYT)-Zimbabwe, Harare, Zimbabwe

^f Department of Plant Production Sciences and Technologies, University of Zimbabwe, Harare, Zimbabwe

^g Unit Subsurface and Groundwater systems, Deltares, Utrecht, the Netherlands

^h Fathom, Bristol, United Kingdom

ARTICLE INFO

Keywords:

Farmers
Irrigation
Senegal
Small dams
Groundwater
PCR-GLOBWB
Modelling

ABSTRACT

Study region: The country of Senegal

Study focus: One consequence of climate change is shifting precipitation patterns towards shorter rainfall regimes, posing challenges to societies relying on agricultural activities. A possible avenue to alleviate the impact of climate change is the construction small-scale reservoirs to locally supply irrigation water for small-holder farmers. Here, we assess the ability of small-scale reservoirs to close the agricultural water gap in Senegal. To this end we introduce a method to find locations and capacities of small-scale reservoirs in a 1 km hyper-resolution global hydrological model that are most effective in minimizing the water gap.

New hydrologic insights for the region: We find that the effect of small-scale reservoirs varies regionally, and that the optimum design does not close the water gap. More locally, the water gap can be reduced during the growing season, indicating that small-holder farmers in vicinity to such reservoirs can benefit. To close the remaining water gap, we assessed the feasibility of groundwater pumping. With pumping, the water gap can be closed, yet often only at the expense of sustainable groundwater use. Due to the novelty of the methods presented, this study should not provide any input to actual decisions. It shows, however, the potential of using hyper-resolution hydrological models for small-scale analyses. More practically, it highlights the immense challenges for societies affected by the climate crisis to meet their water demand in a sustainable way.

1. Introduction

Climate change will affect precipitation patterns, volumes and intensities and has a marked influence on temperature. As a

* Corresponding author at: Fathom, Bristol, United Kingdom.

E-mail address: j.hoch@fathom.global (J.M. Hoch).

<https://doi.org/10.1016/j.ejrh.2024.102074>

Received 23 April 2024; Received in revised form 6 November 2024; Accepted 8 November 2024

Available online 26 November 2024

2214-5818/© 2024 The Author(s).

Published by Elsevier B.V. This is an open access article under the CC BY license

(<http://creativecommons.org/licenses/by/4.0/>).

consequence, floods and droughts are expected to occur more frequently (Ranasinghe et al., 2021) with potentially detrimental societal and economic effects. Regardless of changing climate, in the past the Sahel region has already faced disastrous droughts in the 1970s and 1980s, leading to famine and soil degradation (Bernards, 2021; Ilboudo Nébié et al., 2021).

Senegal is only one example where the effects of climate change are already apparent (IFPRI, 2013): rainfall has decreased by 30 % between 1950 and 2000 (Leippert et al., 2020) and is expected to decrease up to another 10 % by 2040 (Gutiérrez et al., 2021). Temperature has increased by 1.6 °C (McSweeney et al., 2010) and may further increase by 1.0 °C in 2040 compared to the reference period of 1995–2014 as projected under RCP 8.5 according to CORDEX Africa. Altogether, the length of the rainy season may decrease by four days around 2030 and by one to three weeks in 2040–2069 (Araya et al., 2022; Kumi and Abiodun, 2018). Without mitigation and adaptation measures, future droughts will likely be disastrous: already in 2002 and 2011, 200,000 to 800,000 people faced food insecurity due to droughts (Leippert et al., 2020). During the 2002 drought, groundnut yields declined by 75 % and millet/sorghum yields by 60 % (GFDRR, 2011), resulting in a loss of 217 million USD, or 33 % of the agricultural production value (D'Alessandro et al., 2015). Less stable food production also increases the dependency on the international market for food import. Declining levels of food self-sufficiency in rural areas and higher temperatures can furthermore trigger urbanisation and migration (Bernards, 2021; de Bruijn et al., 2024; Oya and Ba, 2013).

In Senegal, the agricultural sector contributes 17 % of the GDP (Leippert et al., 2020). Smallholder farms cultivating rain-fed crops constitute more than 95 % of Senegal's agriculture and employ 70 % of the population (Leippert et al., 2020). Cash crops such as groundnuts account for 27 % of Senegal's exports, but smallholder farmers also grow crops for their sustenance (CIAT and BFS/USAID, 2016). Since the majority of the population depends on agriculture for their nutrition and income, failed harvests pose a threat to food security (Ilboudo Nébié et al., 2021). Already now, 70 % of food is imported (CIAT and BFS/USAID, 2016; Escobar et al., 2022). The main driver of low agricultural productivity is in fact low nutrient input (Affholder et al., 2013). Poor quality of seeds and inadequate farm practices and infrastructure also drive low nutrient use efficiency and low fertilizer profitability (Jayne et al., 2018; Vanlauwe et al., 2014). Climatic factors such as erratic rainfall, floods, and droughts further constraint the sustainable intensification of cropping system in this type of semi-arid area (Falconnier et al., 2020). Droughts in Senegal are characterised by a delayed onset and shorter duration of the rainy season (GFDRR, 2011) – all of which rain-fed crops are sensitive to, which creates a great risk of negative returns on investments for farmers who want to intensify their cropping systems with more nutrients (Ricombe et al., 2017).

Irrigation of currently rain-fed crops could help alleviate water stress both now as well as in the future and help cushion farmers against the risk related to intensification of cropping systems. In Asia, for instance, the increase in irrigated areas has significantly boosted food production (Hussain and Hanjra, 2004). Furthermore, simulations indicate that millet yields in Senegal increases under irrigated conditions compared to rain-fed conditions under projected climate scenarios at the majority of stations up to around 20 % (Araya et al., 2022). Implementing irrigation systems not only reduces water stress (Pavelic et al., 2013) but also would mitigate plant heat stress. For instance, Lobell et al. (2011) found that African maize growth is highly sensitive to temperature increases, resulting in yield declines of 1.7 % for every degree above 30 °C under dry conditions. However, under irrigated conditions, this decline could be reduced to 1 %.

To facilitate the implementation of irrigated agricultural systems, the Senegalese government has constructed large dams in the Senegal River. However, the revenue generated from these large infrastructure projects is low compared to the substantial investment costs since inefficient irrigation schemes as well as side-effects such as health problems caused by stagnant water and land degradation resulting from these schemes, have led to unanticipated costs (Manikowski and Strapasson, 2016).

In contrast to such large-scale water infrastructures, small-scale irrigation systems may offer a more sustainable and inclusive solution to mitigate water deficits during the growing season (Laube et al., 2008). First of all, the small-scale infrastructure can be managed by local communities, depending on their needs (Acheampong et al., 2018). Furthermore, small-scale systems have a lower local environmental impact compared to large-scale systems (Owusu et al., 2022).

Additionally, these small-scale irrigation systems have shown great potential in alleviating poverty (Hussain and Hanjra, 2004). In Burkina Faso, for example, small reservoirs and small-scale irrigation systems such as buckets, watering cans and motorised pumps used to irrigate rice and vegetables, have increased the additional dry season income with 200–600 USD per individual household (Giordano et al., 2012). This additional income not only enhances food security but also provides opportunities for healthcare, education, and farm investments (Giordano et al., 2012).

Given that the majority of agricultural land in Senegal relies on rain-fed farming, implementing small-scale irrigation potentially improves water availability during times of water shortage and droughts (Acheampong et al., 2018), provided crop yield is not nutrient-limited (Falconnier et al., 2020). According to Namara et al. (2011), small reservoirs and permanent shallow groundwater irrigation have proven to be most effective in reducing food insecurity among smallholder farmers compared to other small-scale irrigation techniques. In Senegal, the estimated volume of available renewable groundwater is 3.5 km³ year⁻¹, of which only 21 % is currently abstracted (Cobbing and Hiller, 2019). Groundwater has been identified as a potential reliable water source in regions which are highly sensitive to erratic rainfall patterns (ANACIM, 2014). In addition, irrigation by small reservoirs in Senegal is highly underdeveloped according to available literature: Owusu et al. (2022) listed only one small reservoir in Senegal.

Even though these studies suggest that small reservoirs and groundwater pumping may have the potential to improve the water availability for smallholder farmers, thus far only two studies modelled the irrigation potential in Senegal in more detail. Altchenko and Villholth (2015) mapped the percentage of land that could be equipped for groundwater irrigation but considered a fully irrigated harvest during the dry season. However, they did not consider the option of small scale reservoirs. Furthermore, their model did not incorporate lateral groundwater fluxes, whose inclusion makes groundwater simulations, particularly when considering pumping, likely more realistic (de Graaf et al., 2019). The second study by Xie et al. (2014) assessed the potential of both groundwater irrigation and small reservoirs but did not incorporate a decadal timespan, which is essential to account for natural variability and the time

required for the groundwater to reach equilibrium state. While elucidating the potential of small-scale irrigation techniques, these studies have not explored the combined effect of small reservoirs and groundwater pumping, resulting in a knowledge gap regarding their combined irrigation potential.

Aiming to advance our understanding of the hydrological effectiveness of small-scale water infrastructure projects, we here address the following research questions: *i*) to what extent can small reservoirs fill the current water gap?; and *ii*) to what extent can groundwater pumping fill the remaining water gap after implementation of small reservoirs? To address these questions, we use the global hydrological and water resources model PCR-GLOBWB 2.0 (Sutanudjaja et al., 2018) as it accounts for both surface water and groundwater processes, reservoir dynamics, and irrigation water demand. The recently developed version at 30 arc-seconds spatial resolution (Hoch et al., 2023; Verkaik et al., 2022) now provides the spatial detail required for such case studies. By employing a global model together with globally available datasets and a novel generic workflow drawing from both engineering and scientific literature, the here proposed approach and results should not only give us better insights how smallholder farmers may become more climate resilient, but also provide a tool for similar analyses in other hotspots.

2. Study area: Senegal

2.1. Geography

North and central Senegal is located in the Sahel with the Atlantic Ocean forming the western border of Senegal. Senegal is divided into fourteen regions (Fig. 1A). Dakar is the capital of Senegal and seen as a separate region. The regions of Ziguinchor, Sédhiou, and Kolda combined are referred to as Casamance.

2.2. Socio-economy

In 2021, the population of Senegal was estimated to be 16.9 million people, compared to 9.7 million in 2000 (World Bank, World Development Indicators, 2021b), a significant population growth. Approximately 42 % of the population is younger than 15 years, and 97 % is younger than 65 years (World Bank, World Development Indicators, 2021b). Around 9.3 % of the population lives below the poverty line (World Bank, World Development Indicators, 2018), and the Gross Domestic Product (GDP) is reported to be US\$27.6 billion (World Bank, World Development Indicators, 2021a). As a consequence of droughts during the 1970s and 1980s, the GDP declined from 1982 until 1994 (Sow et al., 2016).

2.3. Climate

Senegal's climate can be categorised into three zones: arid in the North, semi-arid in the central part, and tropical savannah in the South (Onojeghuo et al., 2017). This is also visible from the precipitation data used in this study (Fig. 14A). The arid and semi-arid areas are part of the Sahel region (Leippert et al., 2020). Precipitation strongly depends on latitude and season: from more than 1200 mm/year in the South to less than 200 mm/year in the North. The rainy season in the South ranges from June to October, while the shorter rainy season in the North occurs from July to September, followed by a dry season between November and June (Leippert et al., 2020; McSweeney et al., 2010). Fig. 14B displays the average monthly temperature as used to force the model. Average temperatures range below 27 °C at the Coast and increase to above 30 °C towards the East.

2.4. Surface water

Two major river basins are present in Senegal: the Senegal River Basin and the Gambia River Basin (Fig. 1B). The Senegal River originates in Mali and enters Senegal approximately 200 km further downstream. The total area of the Senegal River catchment is around 483,200 km² (Finger and Teodoru, 2003) and its monthly mean discharge varies between 300 and 1000 m³/s and highest mean discharges occurring in the months September-November.¹

The Gambia River flows through Senegal to the Gambia, where it eventually reaches the Atlantic Ocean. It also originates in the Fouta Djallon Mountains in Guinea (Degeorges and Reilly, 2006) and enters Senegal in Kédougou (Magatte et al., 2005). The size of the Gambia River catchment area is approximately 77,000 km² (Lamagat et al., 1990). Its monthly mean discharge varies between 50 and 300 m³/s with highest discharge recorded in the months August-October.²

In addition to these major rivers, the Casamance River can be found in Casamance. Due to its low flow rate, saltwater intrusion occurs in this river until the Sédhiou region. Similar natural processes and factors such as elevation, distance to river, land use, and soil properties are leading to salinization in the Sine and the Saloum, flowing through the Louga, Diourbel, Fatick, and Kaolack regions. As a result of the salinization, the quality of soil and agricultural productivity has declined particularly in areas near these rivers (Thiam et al., 2019).

¹ According to GRDC records from 1903 to 1974 at station Dagana.

² According to GRDC records from 1970 to 1994 at station Gouloumbou.

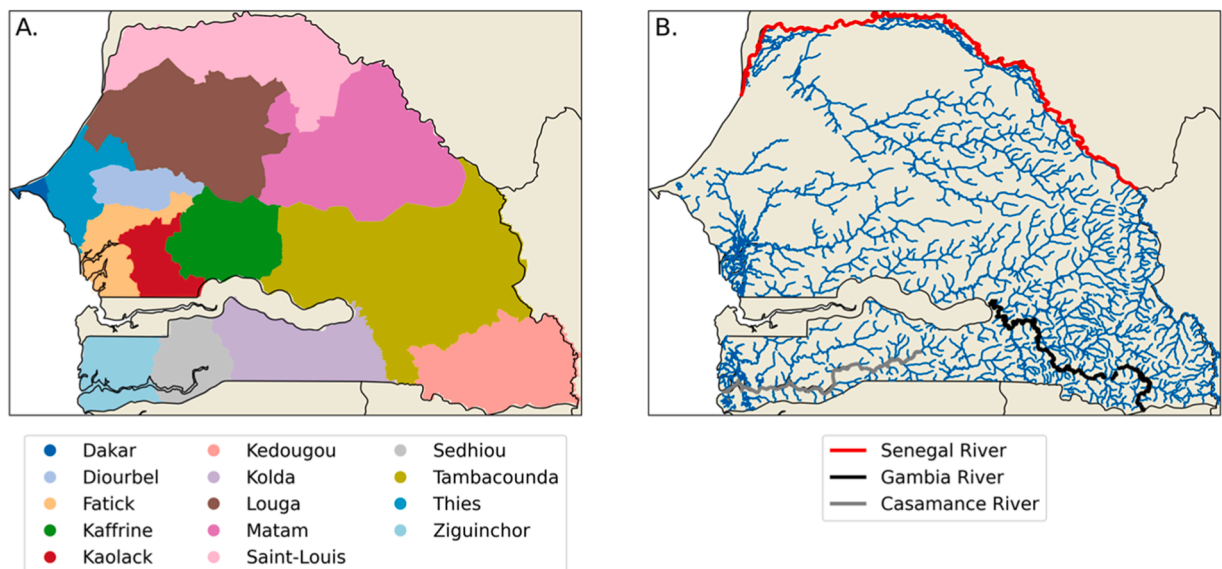


Fig. 1. A.) The fourteen Regions of Senegal. Adapted from Hijmans (2015); B.) Map of all the rivers in Senegal. Obtained from ISCGM/DTGC (2012).

2.5. Hydrogeology

Groundwater in Senegal is distributed among four aquifer systems: the superficial, intermediate, deeper, and basement aquifers (USAID and SWP, 2021). The superficial aquifer is a collection of several smaller aquifers consisting mainly of sand and sandy clay (Madione et al., 2018). The amount of groundwater abstraction for irrigation in this upper aquifer varies across regions, from non-productive in Thiès to 80 m³/h in Tambacounda (Senagrosol, 2009).

The intermediate aquifer is primarily composed of limestone, characterised by karsts and faults (Bense et al., 2013; Madione et al., 2018). The Palaeocene formation within the intermediate system is not productive in the Diourbel region, but the yields for the entire aquifer could reach up to 50 m³/h in Tambacounda (Senagrosol, 2009).

The deep aquifer system, known as the Maastrichtian formation (Senagrosol, 2009) covers 80 % of the country and consists of sand, sandy-clay, and calcareous sandstone (Madione et al., 2018; USAID and SWP, 2021). This system has high productivity, with yields of up to 150 m³/h (Senagrosol, 2009). The basement aquifer system generally has low yields with small patches of volcanic formations having moderate productivity (Madione et al., 2018).

2.6. Agriculture

Rain-fed agriculture predominates in Senegal, with the largest part of agricultural land being cultivated by smallholder family farms (Leippert et al., 2020). Irrigated agriculture is practiced mostly in the Senegal River Valley (SRV) and in Niayes, a coastal strip located north of Dakar (Leippert et al., 2020; Siebert et al., 2013). In Niayes, agricultural practices are more commercialized compared to smallholder farms, with horticulture and intensive livestock farming being the main activities (Faye and Msangi, 2018). Water for irrigation in the SRV primarily comes from the Senegal River, as the region receives limited precipitation.

Other irrigated areas in Senegal are scarce. There, water infrastructure is less developed: motorised pumps, manual lifting, and small artificial ponds are the main means for irrigation (Senagrosol, 2009).

The Groundnut Basin, encompassing the Thiès, Diourbel, Fatick, Kaolack, and Kaffrine regions, is the major cultivation area for groundnuts and millet (Leippert et al., 2020) with crop rotation being the principal cropping system (IFPRI, 2013). Soils in the Groundnut Basin are naturally low in soil organic matter and have a limited capacity to retain nutrients, which has further declined due to agricultural activities (McClintock and Diop, 2005). Other rainfed crops include cowpeas, sorghum, and maize (IFPRI, 2013). Rainfed crops are typically planted at the beginning of the rainy season around May/June, which marks the start of the growing season. The length of the growing season depends on the duration of the rainy season which typically ends in October/November (Araya et al., 2022; see Section 2.3).

3. Methodology

3.1. PCR-GLOBWB 2 description

Simulations were performed using PCR-GLOBWB (hereafter PCR) (Sutanudjaja et al., 2018), a global hydrological and water

resources model. The model consists of two vertically stacked soil layers and accounts for various vertical fluxes between sub-surface, surface, and atmosphere. Important for the study here is that PCR incorporates reservoir dynamics, as well as human water demands for irrigation, livestock, industry, and households. Water withdrawal for irrigation depends on the crop water requirements, which vary according to crop type and stage of development (Sutanudjaja et al., 2018). Due to the small size of reservoirs (Stephens, 2010) and the point nature of groundwater pumps, the recently developed 1 km version of PCR (Hoch et al., 2023; van Jaarsveld et al., 2024) was applied here. If not stated otherwise, we employed the default model parameterisation as described in Sutanudjaja et al. (2018) and Hoch et al. (2023).

3.2. Input data

Simulations covered the period 2000–2019 at a daily time step. Except for discharge, all output variables were reported as monthly averages to minimise data storage requirements.

3.2.1. Meteorological forcing

Precipitation input was obtained from the W5E5 version 2.0 dataset, a global dataset covering the period from 1979 to 2019. This dataset provides daily precipitation values at a spatial resolution of 60 arc-minutes (Anon, 2021). To reduce the difference between model resolution and input data resolution, the precipitation data was downscaled to 150 arc-seconds (± 5 km) by means of the Climate Hazards Group InfraRed Precipitation with Stations (CHIRPS) dataset (Funk et al., 2014). For other meteorological variables required to calculate reference potential evapotranspiration such as radiation or wind speed, the ERA5- Land data was used (Muñoz-Sabater et al., 2021). Please see appendix A1 Meteorological input for more information.

3.2.2. Land cover

In the default land cover module of PCR, main agricultural areas in Senegal are predominantly defined as natural vegetation - a relic of coarser input data and model resolution. Consequently, there is no defined cropping season and no seasonality in the crop water requirement in these areas. To obtain accurate estimates of the crop water requirement, the default input for the land cover module was improved with several new datasets, yielding a map of the distribution of crops and their types (Fig. 2). A detailed outline of how this was done can be found in appendix A2 Land cover. The default values in PCR for paddy crops were used as input for flooded and irrigated rice.

3.2.3. Abstraction zones

To meet the irrigation water demand, PCR utilises surface water or groundwater, if available. However, the model limits the distance from which water can be sourced to meet the demand using so-called abstraction zones: water demand within a zone can only be satisfied by cells within the same zone. The default size and shape of these zones depend on watershed and administrative boundaries, with a minimum size of 30 arc-minutes (Sutanudjaja et al., 2018).

In this study, the size of the abstraction zones had to be modified as small reservoirs cannot irrigate an area of 30 arc-minutes (around 50 km² at the Equator). In absence of alternative approaches, a novel approach was devised, relating the size of the abstraction zones with the irrigation water need of Groundnuts during a dry year. Groundnuts were chosen as reference since they are the dominant crop type (Fig. 2), and typically require on average around 600 mm of water (Doorenbos and Kassam, 1979). During the 2002 drought, Kaolack (a major groundnut production area in Senegal) received 390 mm of precipitation (Muñoz-Sabater et al., 2021),

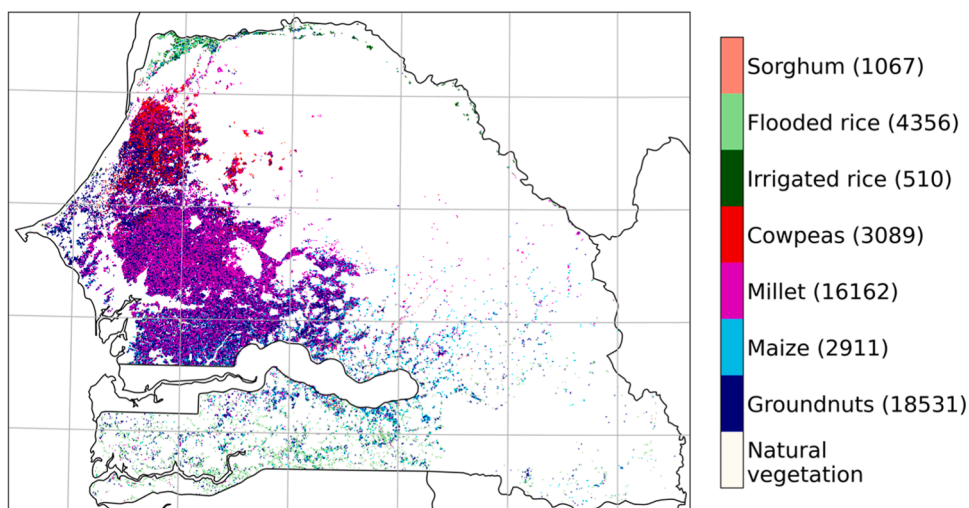


Fig. 2. Map of the principal crops in Senegal. The numbers in the labels indicate the number of cropland cells of the specific crop type.

resulting in a water gap of 210 mm. Using the default irrigation efficiency of 0.7, the required irrigation water is 300 mm. Per hectare, this yields a required irrigation volume of 3000 m³. Considering a small reservoir with a storage capacity of 100,000 m³, an area of 33 ha can be irrigated. Using only one crop and a drought year could be considered as simplistic, but given the lack of other examples to follow, we think that combining the dominant crop with a year where irrigation demand was high, should provide an adequate and conservative estimate of the required size of the abstraction zones.

In Senegal, the surface area of one cell is approximately 100 ha. Thus, one reservoir has the potential to irrigate 0.3 cells. According to [Venot and Hirvonen \(2013\)](#), small reservoirs in the Sahel region can irrigate less than 50 ha, qualitatively confirming that the estimated values of our parsimonious approach are sensible.

3.3. Model validation

The performance of the uncalibrated hydrological model was evaluated by comparing the output of a baseline simulation (i.e., without reservoirs or pumps implemented) with observed data for discharge, soil moisture, and actual evaporation.

Simulated discharge was validated using observed river discharge data from the GRDC database. Unfortunately, only one station within the study area (Pont de Telimele), located in Guinea, provided discharge measurements during the simulation period. The Kling-Gupta efficiency (KGE) was used as an evaluation metric to assess the accuracy of the simulated data compared to the observed data ([Gupta et al., 2009](#)). While data from a single discharge station cannot provide a comprehensive assessment of the model's performance in simulating discharge, it still can indicate whether the model captures periods of high and low flow, main indicators of floods and droughts ([Brunner et al., 2021](#)).

Second, the simulated volumetric soil moisture content (VMC) results were compared per region in Senegal to remotely sensed soil moisture data from the ESA CCI Soil Moisture dataset. This dataset is derived from a combination of satellite data and covers the period from 1974 to 2021 ([Dorigo et al., 2017](#); [Gruber et al., 2019](#)). The spatial resolution is 15 arc-minutes. The ESA CCI Soil Moisture dataset measures soil moisture up to a depth of 5 cm, while PCR considers the first soil layer with a thickness of 30 cm and averages soil moisture over this layer. Due to this difference, absolute VMC values may differ between simulation and observations. Hence, only the coefficient of determination (R²) was used as the validation metric, since it indicates whether the model accurately captures the variability and trends in soil moisture, even if the absolute values differ.

Finally, monthly simulated actual evaporation results were compared per region to the GLEAM dataset, which provides estimates of actual evaporation at a spatial resolution of 6 arc-minutes ([Martens et al., 2017](#); [Miralles et al., 2011](#)). The relative root mean squared error (RRMSE) was used to assess the validity of the simulated actual evaporation, as described in [Hoch et al. \(2023\)](#).

For both simulated VMC and actual evaporation, both observed and simulated cell values are averaged across each region per time step and then R² and RRMSE were computed across all time steps. This yields a metric value per region.

3.4. Reservoir design and implementation

In absence of a blueprint to design and implement small-scale reservoirs, we drew on both engineering and scientific literature to produce a novel workflow. The workflow is based on a set of criteria defined in a two-step approach consisting of a topographical and hydrological analysis and tries to combine practitioner insights with latest scientific knowledge. [Fig. 15](#) presents a flowchart outlining the reservoir design process.

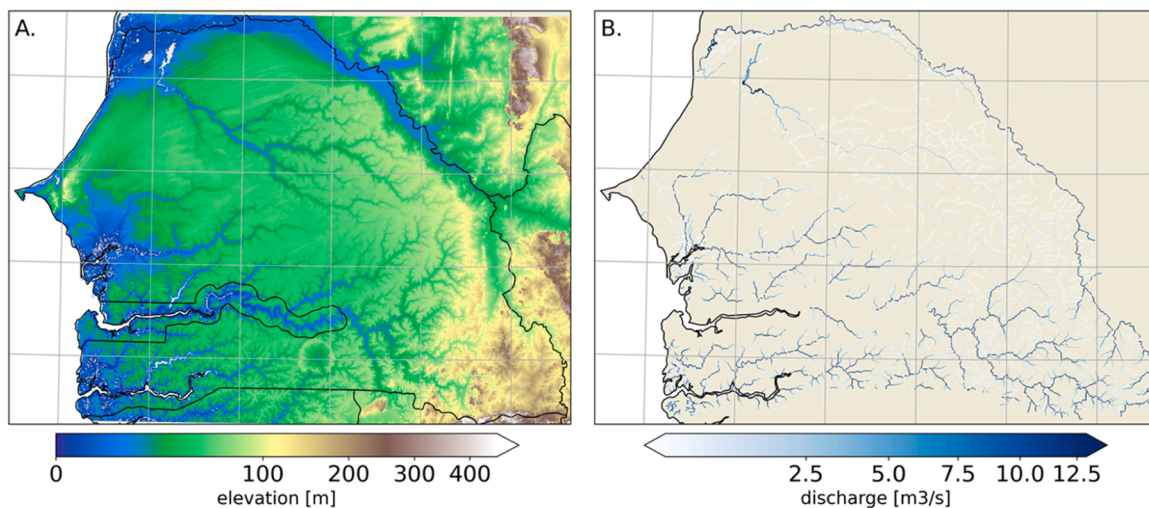


Fig. 3. A.) Digital elevation model (DEM) of Senegal. Original DEM was obtained from [Hawker et al. \(2022\)](#); B.) Average annual total discharge in Senegal over the period 2000–2019, result from the reference simulation.

3.4.1. Topographical analysis

According to [Stephens \(2010\)](#), a maximum dam height of 5 m is advised for small reservoirs. Additionally, two smaller dam heights of 3 m and 4 m were evaluated. Per cell of 30 arc-seconds, the topographical suitability was assessed by clustering a high-resolution 1 arc-seconds bare-earth DEM ([Hawker et al., 2022; Fig. 3A](#)) into blocks of 30×30 cells (which effectively corresponds to one cell of the model's spatial resolution of 30 arc-seconds). Then, by determining the minimum high-resolution DEM value within each block, the dam location in each 30 arc-seconds cell is derived, thereby assuming a dam is located at the lowest possible elevation. By adding the different dam heights to this minimum value, three 'dam height thresholds' were determined. Only if this dam height threshold did not exceed the elevation value of the 30 arc-seconds DEM of PCR, a cell was considered suitable for reservoir construction as a filled reservoir could spill over to neighbouring cells otherwise.

The reservoir volume in one 30 arc-seconds cell was calculated by accumulating across all cells from the 1 arc-seconds DEM that are below the dam height threshold. Similarly, the reservoir area was calculated. This together yielded a map of potential reservoirs meeting the topographical design requirements

3.4.2. Hydrological analysis

To assess the hydrological suitability of these potential reservoirs, the volumes computed in the previous steps were compared to the total annual discharge in each 30 arc-seconds cell ([Fig. 3B](#)).

For each potential reservoir, the total yearly discharge in the cell was divided by the reservoir volume, resulting in a "discharge/volume ratio". An upper and a lower boundary of this ratio was defined within which the reservoir construction is reasonable from a hydrological view. These boundaries prevent reservoirs from completely retaining all discharge, leading to downstream water shortages, as well as avoid situations where high river discharges relative to reservoir volume could damage the reservoir, which could be the case in the Senegal River.

The lower limit of the discharge/volume ratio was set to 0.8 and applied to the five years with the lowest average yearly discharge in Senegal from the reference simulation (see [Section 3.6](#)). As a result, cells were considered unsuitable if the volume of a reservoir exceeded 80 % of the total yearly discharge during any of these five driest years.

Then, to define the minimum volume of potential reservoirs relative to the total yearly discharge in each cell, the upper limit of the discharge/volume ratio was derived through an analysis of the Global Reservoirs and Dam (Grand) database ([Lehner et al., 2011](#)). Note that not all data points in the Grand database were used as we excluded very small and very large dams which are not representative for the present study (see appendix A4 Hydrological analysis). The remaining data points were used to fit an exponential regression function to reservoir inflow and reservoir volume:

$$\frac{\text{discharge}}{\text{volume}} = 2.24 * e^{-0.0160 * \text{volume}}$$

Typical values for the minimum reservoir volume were retrieved from [Stephens \(2010\)](#) and entered into the derived empirical formula. These values are 10,000, 13,333, and 16,666 m³ for dam heights of 3, 4, and 5 m, respectively, yielding a maximum discharge/volume ratio for each dam height from the fitted relationship: 2.2937, 2.2936, and 2.2934. Consequently, reservoirs where the inflow discharge leads to and exceedance of these maximum ratios were excluded.

3.4.3. Reservoir selection

A last step ensured that reservoirs could not cluster along the rivers. Hence, we allowed for only 1 reservoir in each selection area. The size of these areas is based on the observation that many small reservoirs in Burkina Faso are located within a radius of 5 km of each other ([Cecchi et al., 2009](#)). Therefore, the size of the first selection area is 5×5 cells. However, this reservoir density has resulted in conflicts among users ([Giordano et al., 2012](#)) and, moreover, fewer reservoirs may be desirable as they retain less sediment ([Brandt et al., 2017](#)), and impact downstream discharge less ([Owusu et al., 2022](#)). To test the impact of the selection area size, a second selection area was applied with a size of 10×10 cells.

Accounting for evaporation losses is crucial during reservoir design as they can reach up to 75 % of the total volume for small-scale reservoirs ([Mady et al., 2020; Stephens, 2010](#)). To avoid the implementation of reservoirs with a great surface area and hence likely great losses, deep reservoirs with smaller volumes were preferred over shallow reservoirs with larger volumes. Therefore, the surface area of the reservoirs was multiplied by the 20-year average potential evaporation in June as this month marks the beginning of the growing season for non-paddy crops and flooded rice. Arguably, there are many ways to select the most suitable reservoirs. We here decided to consider only one month to determine evaporation losses, assuming that monthly total discharge can at least partially recover them since reservoir volumes are small relative to the inflow discharge. The resulting potential evaporation losses were subtracted from the maximum reservoir volume calculated above.

From the potential reservoirs defined above and after accounting for evaporation losses, the reservoir with the largest volume was selected for each selection area.

3.5. Groundwater pumping implementation

To accurately simulate the effect of groundwater pumping on lateral fluxes, the default groundwater module of PCR was replaced with the two-layer global groundwater model based on MODFLOW ([Felfelani et al., 2021; de Graaf et al., 2019; McDonald and Harbaugh, 1988; Sutanudjaja et al., 2011; Verkaik et al., 2022](#)). To match the 30 arc-seconds spatial resolution of PCR, the default 5 arc-minutes spatial resolution of the MODFLOW module was resampled. It should be noted that the MODFLOW model was not

calibrated due to the lack of appropriate data. To save computational time, PCR and MODFLOW were coupled offline, where recharge and surface water levels from PCR-GLOBWB were used as forcing and boundary conditions to the MODFLOW runs. Furthermore, it needs to be acknowledged that the inclusion of groundwater pumping in the modelling set-up was much less elaborately devised than the reservoir design and selection process. Even though the model default global parameterisation was used, it allows for drawing first conclusions whether groundwater exploitation is an option in Senegal. For the hydrogeological setup and other details about the groundwater modelling we refer to [de Graaf et al. \(2019\)](#).

The rate of groundwater abstraction per 30 arcseconds cell was set to different fractions to the remaining water gap after implementing the reservoir design yielding the largest decrease of the agricultural water gap. We here assume that small-scale reservoirs are the preferred choice to close the water gap and are only supplemented with optional pumping, but arguably other considerations can be made in a real-life setting. The fractions used were 25 %, 50 %, 75 %, and 100 % of the water gap after reservoir implementation. This way, we could model the effect of groundwater pumping at different abstraction rates on groundwater depth. Using different fractions allows for detecting a pumping threshold after which further abstraction becomes unsustainable, that is, abstraction rates that lead to persistent decline of groundwater tables ([Bierkens and Wada, 2019](#)). An alternative approach, which we did not pursue here, is to assess to what extent unutilized replenishable groundwater resource could be utilized by pumps.

3.6. Model simulations

To test the sensitivities and assumptions outlined above, several modelling simulations were conducted ([Table 1](#)).

The first simulation A served as the reference simulation without the implementation of any irrigation techniques. For each dam height of 3, 4, and 5 m, two variations of reservoir density, expressed as variations of the selection area in which one reservoir can be located, were simulated as a high density of reservoirs affects water availability downstream ([de Fraiture et al., 2014](#); [Section 3.4](#)). This yields in total six simulations labelled B.

From these simulations, the one that reduced the water gap most was selected and groundwater pumping at different abstraction rates was introduced ([Section 3.5](#)), forming the simulations labelled C.

4. Results and discussion

4.1. Model validation

First, simulated discharge from the reference simulation was validated ([Fig. 4](#)). The resulting KGE of 0.22 indicates good model performance given the model was not calibrated at all: according to [Knoben et al. \(2019\)](#), a KGE greater than -0.41 indicates informative simulations, since the model exceeds the mean flow benchmark. Overall, simulated discharge underestimates both low and high flows, yet a significant peak in 2001 is simulated, which is not present in the observations. Using a more advanced routing scheme in the model may improve the accuracy of discharge estimations ([Hoch et al., 2023](#)). However, this would significantly increase computation times ([Sutanudjaja et al., 2018](#)). As it is the aim of this study to assess *relative* impact of small-scale measures, the obtained KGE suffices to provide a robust basis for the envisaged analyses. This is fostered by the fact that the seasonality of river flow is reasonably well captured by the model which is probably of even greater relevance for this study since the agricultural water gap is strongly dependant on monthly variations of water availability and irrigation water demand.

The model was also validated against observations of soil moisture ([Fig. 5A](#)). A high R^2 value indicates that the model accurately captures the variability and trends in soil moisture, even if there is a bias between observed and simulated data, e.g., due to the difference in measurement depth ([Section 3.3](#)). The highest correlation between observed and simulated soil moisture is found in the south of Senegal, with R^2 values fluctuating around 0.9. The lowest R^2 values are observed in the central coastal regions, where they range around 0.7. Overall, these values indicate good model agreement with observations across the entire study area, and especially capture seasonality very well.

Last, [Fig. 5B](#) illustrates the relative root mean squared error (RRMSE) scores for the evaluation of simulated actual evaporation.

Table 1

Overview of model simulations: simulations with no irrigation technique (A); with reservoirs with dam heights of 3, 4, or 5 m, selected from areas of 5×5 or 10×10 cells (B); with reservoirs (dam height and size of selection area to be determined), supplemented by groundwater pumping (C).

Simulation	Irrigation technique	Dam height [m]	Selection area [cells]	Pumping capacity
A				
B3.5	Reservoirs	3	5×5	
B4.5	Reservoirs	4	5×5	
B5.5	Reservoirs	5	5×5	
B3.10	Reservoirs	3	10×10	
B4.10	Reservoirs	4	10×10	
B5.10	Reservoirs	5	10×10	
C25	Reservoirs + pumping	-	-	25 %
C50	Reservoirs + pumping	-	-	50 %
C75	Reservoirs + pumping	-	-	75 %
C100	Reservoirs + pumping	-	-	100 %

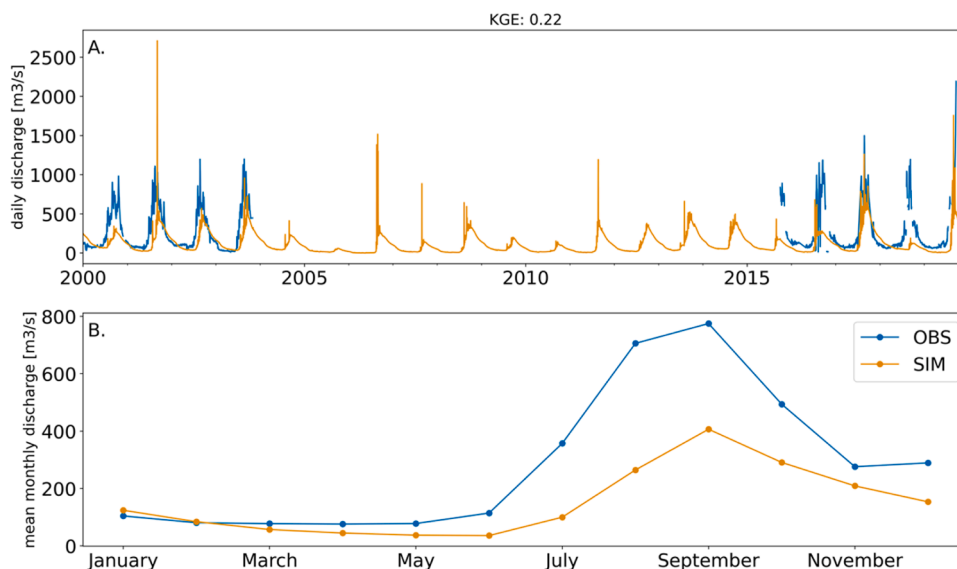


Fig. 4. A.) Simulated and observed discharge at GRDC station Pont de Telimele, located at 10.5°N and 12.9°W; B.) seasonality of mean monthly discharges.

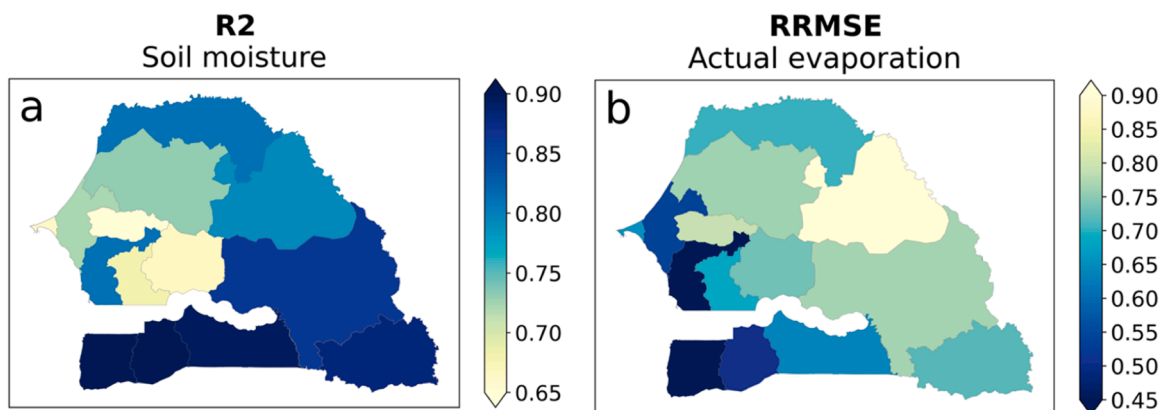


Fig. 5. a) The coefficient of determination (R^2) of the comparison between observed (ESA-CCI) and simulated (reference simulation) soil moisture for the period 2000–2019 in the fourteen regions of Senegal; b) The relative root mean squared error (RRMSE) of the comparison between observed (GLEAM) and simulated (reference simulation) actual evaporation for the period 2000–2019 in the fourteen regions of Senegal.

RRMSE values are lowest in the south and coastal regions, where they fluctuate around 0.5, and gradually increase to approximately 0.8 towards the interior of the country. This pattern appears to correspond with the average temperature pattern (see Fig. 14), suggesting that the model performs better in predicting actual evaporation in areas with relatively lower temperatures. Additionally, the performance of GLEAM in predicting potential evaporation is low in arid regions (Singer et al., 2021), which may further reduce the agreement between simulated and observed values.

4.2. Assessing the reservoir design

To identify suitable reservoir locations and compute their potential volume, a topographical and hydrological analysis was conducted. This section presents the results of these analyses (Fig. 6).

In general, most reservoirs are situated in Casamance, Fatick, Kaolack, Kaffrine, and Tambacounda, as they are main agricultural areas. Hence, only a few reservoirs are in other areas where agriculture is less prevalent. In other areas such as again, as Louga, Thiès, Diourbel, Matam, and Saint-Louis, available discharge determines the (low) number of reservoirs. Reservoirs in simulations Bx.5 and Bx.10 are all located in similar areas, but the reservoir density decreases with greater dam heights and larger abstraction zones, as one would expect. Only in few areas, such as Ziguinchor, reservoir density increases as the dam height increases. This may occur because smaller reservoirs did not pass the reservoir design process, especially the hydrological analysis (Section 3.4.2).

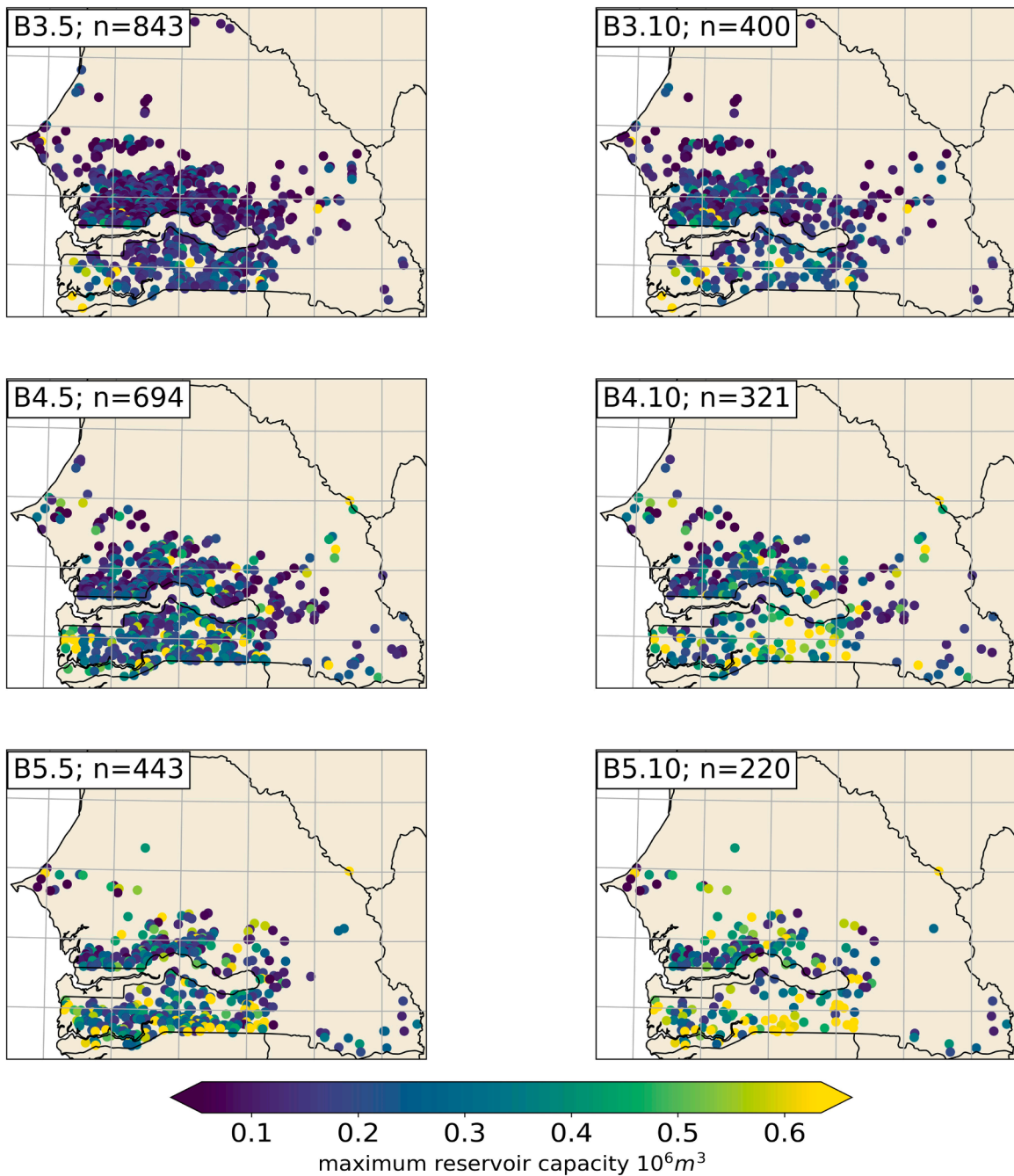


Fig. 6. Locations of reservoirs and their corresponding maximum reservoir capacity for all B simulations, including the number of reservoirs n per simulation.

Fig. 7 displays the maximum reservoir capacity in all B simulations. The maximum capacity is larger for the 10x10 selection area in comparison to the 5x5 selection area for all dam heights, since a larger selection area increases the chance of selecting a reservoir with larger capacity.

According to Owusu et al. (2022), small reservoirs typically have a maximum capacity of up to $10^6 m^3$. Except for a few outliers in simulations B4.5, B5.5, B4.10, and B5.10, the maximum capacity of the reservoirs in the study falls below this value. Furthermore, the majority of small reservoirs in Burkina Faso has a volume between 10^5 and $10^6 m^3$ (Cecchi et al., 2009). Since the reservoir volumes obtained in this study's approach align well, we are confident that the chosen methodology can provide suitable reservoir dimensions.

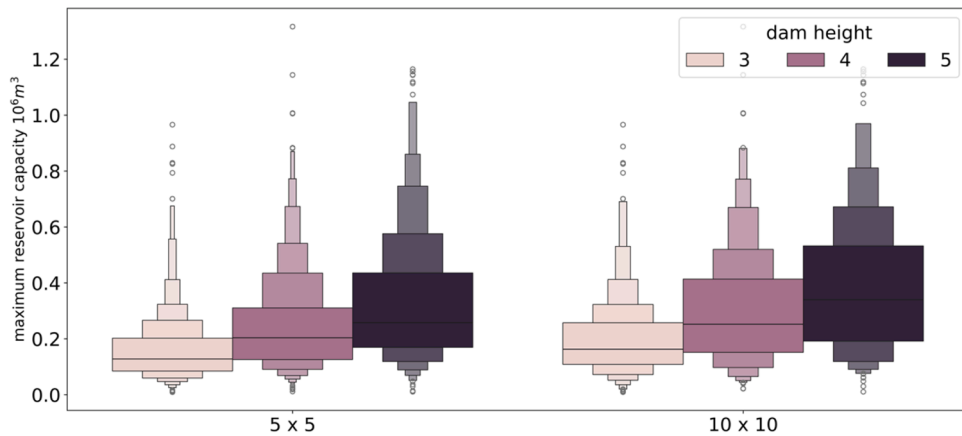


Fig. 7. Box plots of maximum reservoir capacity ($\times 10^6 \text{ m}^3$) implemented in simulations B3.5, B4.5, B5.5, B3.10, B4.10, and B5.10. Reservoirs were designed following a set of rules, based on the topography and hydrology of Senegal. The three left box plots represent a reservoir selection area of 5×5 cells, the three box plots on the right a selection area of 10×10 cells. The dark blue, light blue, and green charts depict dam heights of 3, 4, and 5 m.

4.3. Water gap in the reference simulation

By means of the reference simulation, the benchmark water gap was computed with which all other simulations will be compared (see Fig. 8 and Table 3). Results are in line with expectations and demonstrate that the water gap is determined by the number of cropland cells and precipitation amount in a region (see appendix B1 Reference water gap): in regions where precipitation is low (that is, the North) or the number of cropland cells is high, the water gap is relatively higher than in other regions. Whether or not the simulated water gap is "correct" cannot be assessed independently, but from the validation metrics above in conjunction with the updated data we can assume that the model produces an accurate estimate, given all remaining uncertainties.

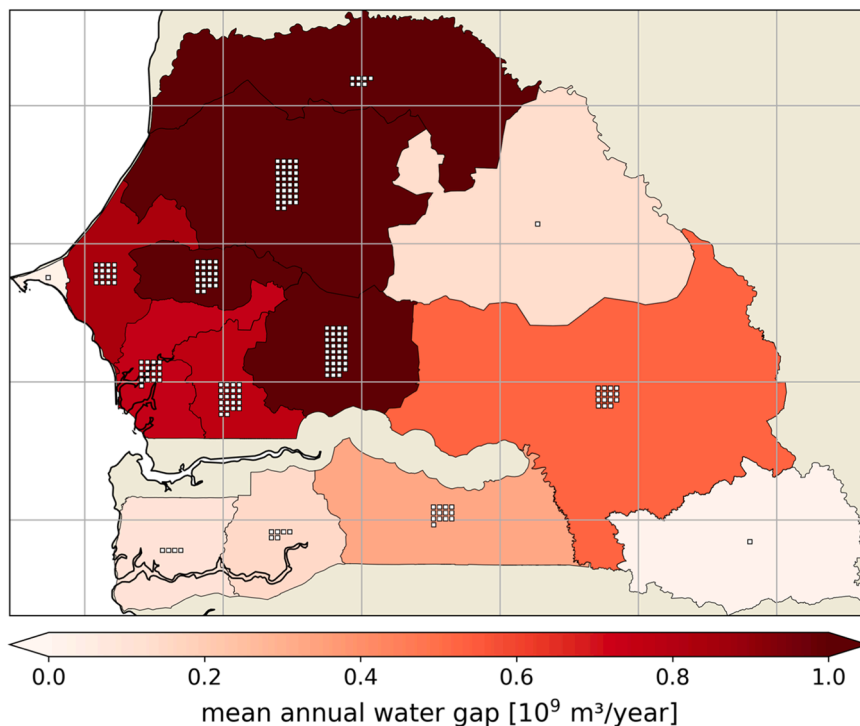


Fig. 8. Mean annual water gap per region in the reference simulation. The water gap is obtained by summing the yearly water gap of all cells in a region, averaged over the period 2000–2019. The number of cropland cells per region is indicated by the white squares. Every square equals 250 cropland cells.

4.4. Reservoir simulations

4.4.1. Regional impact of reservoirs on water availability

To see whether implementation of reservoirs effectively reduced the water gap, the water gap in the B simulations was compared to the benchmark water gap. The percentage decrease in water gap, averaged across region, after implementing the reservoirs is displayed in Fig. 9. Exact values for the decrease in water gap can be found in Table 3.

Overall, the implementation of reservoirs has the greatest impact in Casamance and Kédougou with the largest reduction of 6.27 % occurring in simulation B4.5 in Kédougou. In this region, the total water gap in the reference simulation is relatively low compared to other regions, and there are only a small number of cropland cells to irrigate (Fig. 8). Therefore, a large portion of cropland cells can be irrigated by reservoirs, resulting in a large relative decrease in water gap due to reservoirs.

In Casamance, the reduction in water gap in the individual regions varies per simulation. The reduction in water gap in Casamance shifts to downstream regions with increasing dam height: it peaks in Kolda and Sédhiou in simulation B3.5, while the peak shifts to Sédhiou in simulations B4.5 and B4.10, and finally to Ziguinchor in simulations B5.5 and B5.10. This shift is likely due to the design criteria of the reservoirs: deep reservoirs with a higher dam height have a higher maximum capacity (Fig. 7), requiring a relatively greater annual discharge, and hence they are more likely to be in downstream areas. With fewer reservoirs retaining water upstream (such as in Sédhiou and Kolda), reservoirs in for instance Ziguinchor may result in a greater water gap decrease (Giordano et al., 2012). These results exemplify that, when constructing reservoirs, upstream-downstream links across the entire river basin need to be considered.

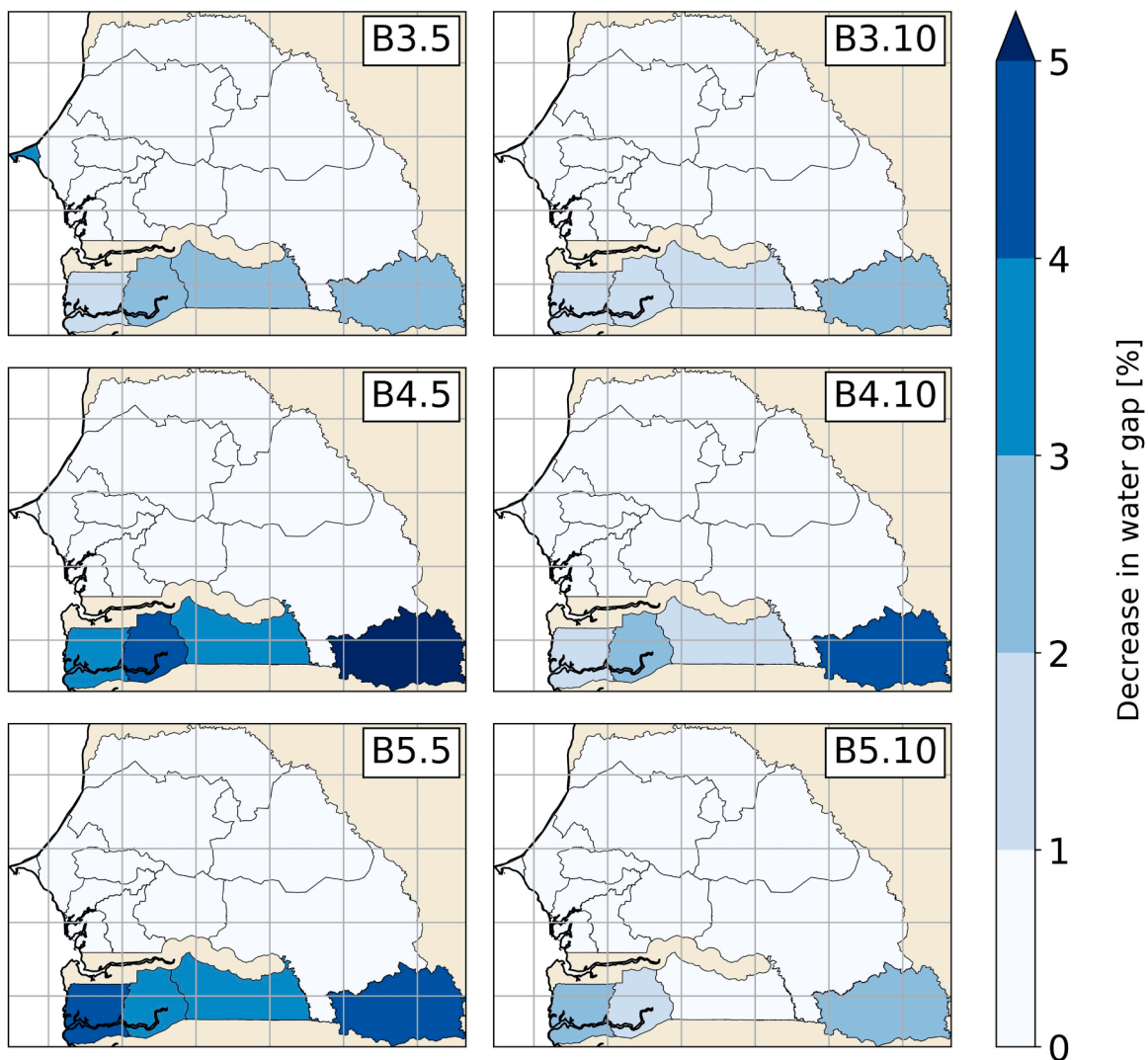


Fig. 9. Decrease in average annual water gap (%) per region after the implementation of reservoirs in all B simulations compared to the water gap in the reference simulation.

It is noteworthy that, in simulation B3.5, the water gap in Dakar decreases by 3–4 %, while in all other simulations it decreases by 0–1 %. This simulation contained a relatively high number of reservoirs in Dakar compared to its surface area, which likely caused the significant decrease in the water gap.

Compared to simulations Bx.5, the decrease in water gap in simulations Bx.10 is smaller. Due to the larger selection area of 10×10 cells, fewer reservoirs are selected, resulting in a smaller area which could profit from reservoirs and in turn in a smaller water gap reduction. This indicates that the study area can accommodate a denser reservoir distribution.

The annual water gap reduction in Senegal in its entirety is provided in Table 2 for both the 5×5 cell and 10×10 cell selection areas in all B simulations. Simulations B4.5 and B4.10 yield the highest decrease in water gap within the respective selection area, suggesting that a dam height of 4 m strikes a good balance between number, spatial distribution, and volume of reservoirs. Overall, simulation B4.5 shows the largest reduction in water gap when aggregated over entire Senegal. Per region, simulation B4.5 performed best in all regions but Fatick, Dakar, and Thiès, indicating that there is likely no global optimum of dam height and selection area.

Since simulation B4.5 has the biggest potential to decrease the water gap, all following analyses are based off this scenario.

4.4.2. Reservoir dynamics

Clearly, not only overall water gap reduction is relevant, but also the temporal impact on the water gap. Fig. 10 displays the monthly water gap (m³) in the reference simulation, alongside the monthly decrease in water gap (%) after the implementation of reservoirs in simulation B4.5 for main agricultural regions in Senegal.

As expected, the agricultural water gap is negligible in the dry season from January to May due to no or hardly any agricultural activities. It starts to increase at the beginning of the rainy season which also corresponds to the growing season for all crops except irrigated rice. The water gap peaks in June to July, and then gradually decreases as the rainy (growing) season progresses, likely due to increased precipitation. Regions where the water gap peaks later in time receive less precipitation at the start of the growing season and hence the water gap builds up. Once the growing season is over in October, the water gap is around zero again.

Interestingly, although the water gap is close to zero from November to May due to the end of the growing season of all crops except irrigated rice, a reduction in water gap is visible from March to May in Kaolack, Kaffrine, and Kolda, with the decrease in April reaching almost 70 % in Kolda. This can be attributed to those cells classified as irrigated rice. These results indicate that the construction of small-scale reservoirs may also be beneficial for other crops with different cropping cycles, if the water demand is not exceeding reservoir capacity and hampering water availability in the next "main" cropping cycle.

The peak water gap reduction coincides with the water gap peak and occurs in June in Sédhiou and Kolda, with the maximum water gap reduction being around 6 % in Kolda in June. For the other regions, water gap reduction remains marginal when assessed across the entire region.

To assess the fidelity of these results, we assess the monthly discharge, monthly water withdrawals, and the reservoir storage at the end of each month (Fig. 11). To prevent reservoir spills, the model regulates reservoir outflow in such a way that the reservoirs are filled to a maximum of 70 % of their maximum capacity. As one could expect, discharge flowing out of the reservoirs increases with reservoir size and more water is released as the rainy season progresses.

Irrigation water withdrawals are zero during the dry season, when no crops are planted. It is greatest in June and July, the first two months of the growing season as the water gap is then at its peak (Fig. 10). Additionally, another peak is visible in September for the 75th percentile of medium and large reservoirs. This peak may be the result of an occasionally occurring lack of discharge, but no definitive answer can be given at this stage.

From January onwards, storage levels start to decline, mostly due to evaporation losses: since the planting of irrigated rice begins in March and only happens in a very limited area, this factor can be ruled out. Intuitively, the lowest storage levels are observed at the beginning of the growing season in June and July when irrigation water withdrawal is peaking. Storage in the reservoirs starts to recover in August when precipitation, and therefore discharge, are increasing. At the end of the year, after withdrawals have stopped, reservoir storage is fully recovered. The fact that reservoir storage is never zero indicates that inflow discharge can balance both withdrawals during the growing season and evaporation losses before the growing season, thereby validating an important assumption made in the reservoir design process (see Section 3.4.3).

Noteworthy, the Penman-Monteith method is used in PCR to compute evaporation which has been found to overestimate actual evaporation from reservoir surfaces compared to in-situ measurements (Owusu et al., 2022). Therefore, evaporative losses from reservoirs may be overestimated and potentially more water could be available for irrigation. Nevertheless, the reservoirs implemented react as intended to natural and human processes such as evaporation and water withdrawal, respectively. As such, simulated magnitude and especially temporal dynamics of water gap reduction can be deemed accurate within the overall uncertainty.

Table 2

Annual average water gap (m³) after the implementation of reservoirs in all B simulations as well as the relative reduction of the reference water gap expressed as percentage.

	5×5 cells		10 x 10 cells	
3 m	3.09×10 ⁷ m ³	0.30 %	1.43×10 ⁷ m ³	0.14 %
4 m	4.03×10 ⁷ m ³	0.39 %	1.81×10 ⁷ m ³	0.18 %
5 m	2.57×10 ⁷ m ³	0.25 %	1.19×10 ⁷ m ³	0.12 %
Reference	1.02×10 ¹⁰ m ³			

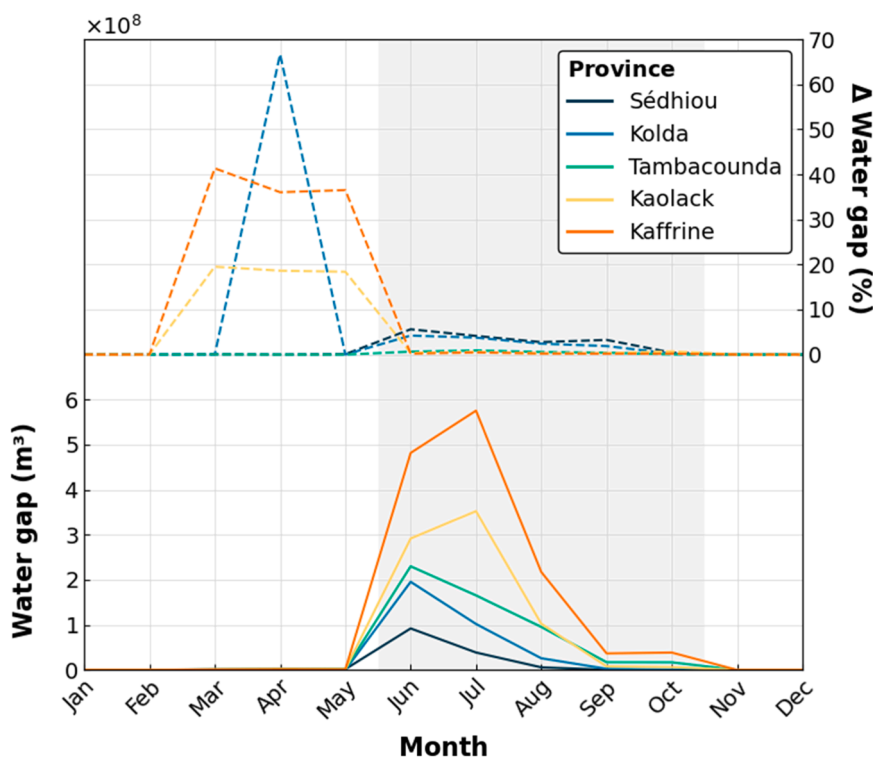


Fig. 10. The total monthly water gap (m³) (solid lines) in the reference simulation, averaged over the period 2000–2019, in Sédhiou (dark blue), Kolda (light blue), Tambacounda (green), Kaolack (yellow), and Kaffrine (orange), the regions in Senegal containing the highest number of reservoirs in simulation B4.5. The dashed lines present the decrease in total monthly water gap (%) after the implementation of reservoirs in simulation B4.5. The grey plane represents the rainy season, which also corresponds to the growing season for all crops except irrigated rice. Monthly values are computed by averaging the water gap and delta water gap per month in the period 2000–2019.

4.4.3. Local impact of reservoirs on water availability

Analysing water gap reduction at the regional level has one main limitation: only a fraction of cropland cells is located within the abstraction zone of a reservoir and can thus be irrigated. Looking at region-wide results, one could conclude that the implementation of small-scale reservoirs is not a viable solution. However, reservoirs may very well be valuable for neighbouring rural communities (Saruchera and Lautze, 2019). Therefore, the analysis was refined to cropland adjacent to reservoirs in the regions of Kaolack and Sédhiou as both regions are agricultural regions with a significant number of reservoirs implemented.

To that end, we compared the water gap in non-irrigated cropland cells adjacent to a reservoir with the reduction in water gap in irrigated cells of the same crop type, adjacent to the same reservoir (Fig. 12). Only reservoirs in Kaolack and Sédhiou that met the requirement of having one cell of the same crop type within their abstraction zone and one adjacent cell outside their abstraction zone were selected for this analysis. In this way, the difference in water gap between irrigated cells and non-irrigated cells could be assessed.

In both Kaolack and Sédhiou, the water gap generally peaks in June or July, the first two months of the growing season (irrigated rice is rare in these regions). The height of the peak is influenced by precipitation and potential evaporation. When precipitation is low, such as during a late onset of the rainy season, or when evaporation rates are high, the water gap reaches its peak (Doorenbos and Kassam, 1979). The water gap starts to decrease when precipitation exceeds potential evaporation, as observed in Kaolack in 2011. In this year, the water gap peaks in July at 0.75×10^5 m³ and decreases to 0.25×10^5 m³ in August, when precipitation peaks. Despite the precipitation exceeding potential evaporation in this month, the water is utilised by the crops and to replenish soil moisture (Doorenbos and Kassam, 1979), resulting in a water gap.

Overall, the impact of reservoirs on the water gap is more significant in Sédhiou than in Kaolack. For instance, in 2013, with minimal precipitation in June at the start of the growing season, additional water available via reservoirs reduced the water gap by 56 % in Sédhiou but only 9 % in Kaolack. The low reservoir performance may be attributed to the higher average maximum reservoir capacity in Sédhiou. Reservoirs in Sédhiou generally reach 70 % of the reservoir capacity each year, as regulated by PCR, while in Kaolack, they usually reach less than half of the reservoir capacity. As a result, more water is available for irrigation in Sédhiou, leading to a greater reduction in the water gap.

It is unclear why cells are not irrigated in June in Kaolack in some years, as the water gap already starts to rise during that month. As there are multiple possible reasons, we can only hypothesize: first, the unfulfilled reservoir capacity as mentioned above; second, higher losses due to evaporation before the start of the growing season; third, the high density of reservoirs in Kaolack, causing upstream reservoirs to retain water from the downstream reservoirs (Giordano et al., 2012); fourth, the potentially small water volume

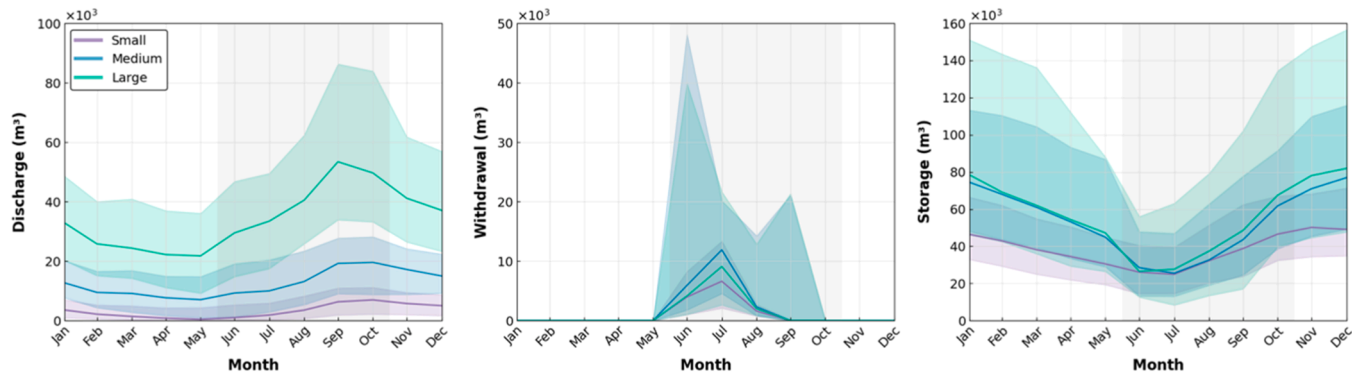


Fig. 11. Reservoir monthly discharge (left), monthly water withdrawals (centre), and reservoir storage (right) at the end of the month, in small (purple), medium (blue), and large (green) sized reservoirs. Reservoirs were categorised based on maximum reservoir capacity. This categorisation was determined by taking the 33rd percentile for small reservoirs, the 67th percentile for medium reservoirs, and the 100th percentile for large reservoirs. The continuous line presents the median monthly values, averaged over the period 2000–2019. The shaded areas indicate the 25th and 75th percentiles for each reservoir size. The grey plane represents the rainy season, which also corresponds to the growing season for all crops except irrigated rice.

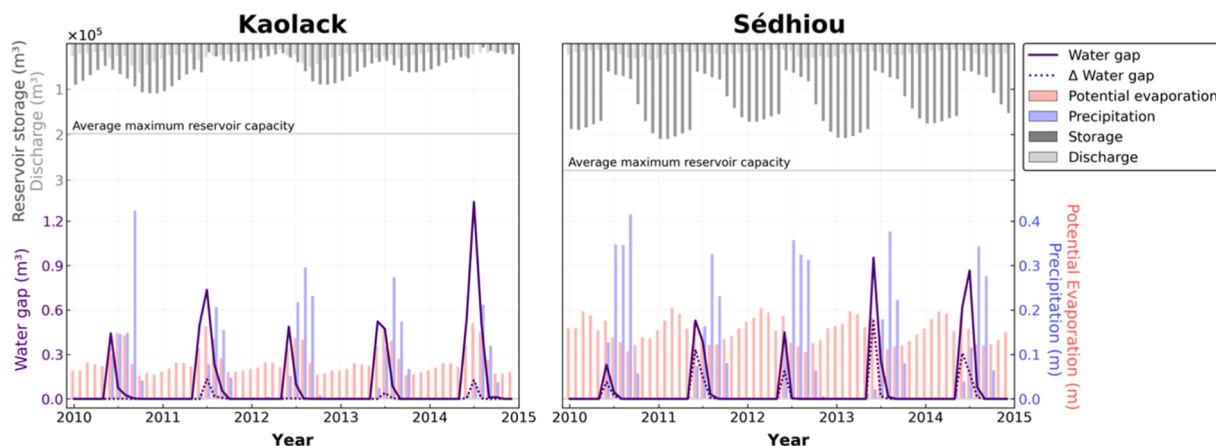


Fig. 12. Reservoir dynamics in simulation B4.5 in Kaolack and Sédhiou in the period 2010–2015, averaged over reservoirs holding irrigated and non-irrigated cells of the same crop type in its 3×3 window. The solid purple line presents the monthly water gap (m^3) in a non-irrigated cell. The dashed purple line presents the difference in water gap between this cell and a neighbouring cell covered by the same crop type, irrigated by a reservoir. The red bars represent potential evaporation (m), averaged over the region, while the blue bars present precipitation (m). The dark grey bars display the reservoir storage (m^3) at the end of each month, averaged over the selected reservoirs, the light grey bars depict the discharge (m^3) out of the reservoirs. The grey horizontal line indicates the average maximum reservoir capacity for the selected reservoirs. It is important to note that the scales of the water gap and precipitation/evaporation are not related.

remaining in the reservoirs has to be used to meet environmental flow requirements; last, the agricultural intensity around reservoirs in Kaolack is greater. In fact, the mean number of cropland cells in the abstraction zone of a reservoir is 2.84, versus 1.72 cells in Sédhiou. Note that the maximum value possible in our modelling approach is 3. Due to the complex interplay between these factors, pinpointing to one specifically is not possible. What can be said, still, is that there are significant inter-annual variations in water gap reductions as well as differences across regions.

4.5. Groundwater pumping

A significant water gap was still left after the implementation of reservoirs, even in simulation B4.5 which resulted in the largest water gap decrease. Therefore, groundwater pumping was simulated as an additional option to close the remaining water gap. Different pumping rates were assessed, ranging from 25 % to 100 % of the remaining water gap after reservoir implementation in simulation B4.5 (Fig. 9). These simulations demonstrate what could happen if farmers chose to entirely or partially close the water gap by means of groundwater pumping. Since MODFLOW was not calibrated for this study but the global default parameterisation was used, the uncertainty of MODFLOW output should be acknowledged.

Fig. 13 and Table 3 show how the depth of the groundwater table (m) changes when groundwater is extracted for a representative cell in a region. For regions with a low diversity in crops this is more likely to be true, while in other areas the effect of pumping may fluctuate more. Unless stated otherwise, the main findings in this section are based on simulation C100, i.e., the simulations where the entire remaining water gap is closed using groundwater.

In most regions, the groundwater table experiences a slight drop each year, followed by recovery. This pattern is likely due to groundwater abstraction at the start of the rainy season in June and recharge at the end of the rainy season in October. Almost everywhere but especially Dakar, there is a significant drop of 3 m in the groundwater table during the drought of 2002 which becomes smaller as the pumping rate decreases. Seeing the intra-annual patterns as well as the impact of the 2002 drought on groundwater table increases our trust that the simulated processes can relatively accurately represent the relevant processes.

In areas where fluctuations of the groundwater depth are small, groundwater withdrawal and recharge are in balance. This could occur when the water gap was already low, resulting in low abstraction rates required to close the gap. Also, areas where precipitation is abundant and groundwater recharge is high can accommodate higher abstraction rates without further lowering the groundwater table. Where the groundwater depth decreases, it may be possible to close the remaining agricultural water gap entirely using pumping.

In instances where the groundwater depth increases, results indicate that the remaining agricultural water gap can only be closed unsustainably. Based on the C100 simulation, there are five regions where this is the case. In these regions, only 25–50 % of the remaining agricultural water gap can be closed in a sustainable way. For the then still remaining water gap, other solutions need to be considered, or a declining groundwater table must be accepted. From a more practical point of view, ever increasing groundwater depths mean that farmers would have to scale the pumping depth of pumps accordingly, possibly resulting in a vicious circle.

It is noteworthy that in Kaffrine and Saint-Louis the groundwater depth starts to increase again around 2012 after an initial recovery. This points to the important link to variations in water availability. In times of low precipitation amounts, discharge is too low to provide sufficient reservoir inflow and recharge is insufficient to sustain the groundwater table in these regions (Comité de Pilotage

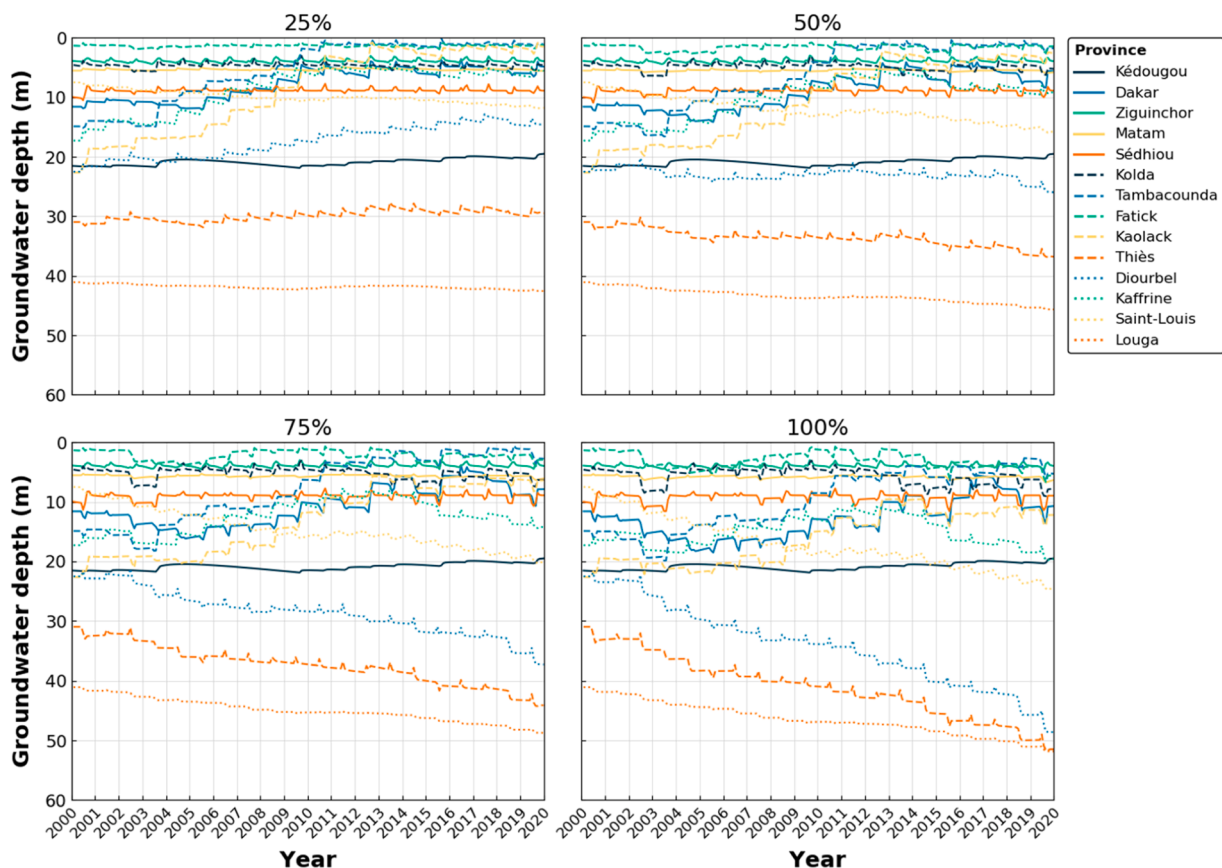


Fig. 13. Groundwater depth (m) in the fourteen regions of Senegal during the study period of 2000–2019. The data is extracted from a cell within an agricultural area in each region, assuming they are representative for all agricultural cells in a region. The regions in the legend are sorted in ascending order based on the total yearly water gap. The figure consists of four panels depicting different scenarios of groundwater pumping at various abstraction rates: 25 % (upper left), 50 % (upper right), 75 % (lower left), and 100 % (lower right) of the water gap that remains after the implementation of reservoirs in simulation B4.5.

Table 3

Groundwater depth in meters across the different regions under the different pumping scenarios at the beginning and end of the simulation period.

	GW depth 2000	GW depth 2019 – 25 %	GW depth 2019 – 50 %	GW depth 2019–75 %	GW depth 2019–100 %
Kedougou	21	19	19	19	19
Dakar	12	4	5	8	12
Ziguinchor	3	3	3	3	3
Matam	5	5	5	5	6
Sedhiou	10	8	8	8	8
Kolda	4	4	5	6	7
Tambacounda	15	2	3	3	5
Fatick	2	2	3	3	5
Kaolack	22	2	3	5	13
Thies	31	30	36	44	52
Diourbel	22	14	26	37	48
Kaffrine	17	5	8	14	19
Saint-Louis	7	12	15	20	25
Louga	41	43	46	48	52

du Livre Bleu Sénégal, 2009). Even though these regions seem to have the capacity to bounce back after dry periods, projected lower precipitations amounts will make this increasingly difficult in the future.

5. Conclusion and recommendations

We evaluated the feasibility of using small-scale reservoirs and groundwater pumping to reduce the water gap in Senegal for small-

holder farmers. Due to a lack of generic blueprints for such a study, we leveraged on available global and local datasets as well as both engineering and scientific literature to design a reusable workflow to design these reservoirs.

To our pleasant surprise, the reservoir dimensions computed with the novel approach agree well with reference values. Furthermore, we find that seasonal reservoir dynamics are realistic and hence allow for drawing a first set of conclusions.

At large, the results indicate that only a combination of reservoirs and groundwater pumping may close the water gap required to fully irrigate rain-fed agriculture in case insufficient rainfall is available. In none of the regions, reservoirs alone were able to close the water gap. However, by zooming in from the regional scale to the local scale, the local impact on water availability can still be significant, although this differs across regions. For example, in Sédhiou, additional irrigation water from reservoirs reduced the local water gap up to 56 % during a dry year. While this is good news, results at large indicate that reservoirs alone cannot reduce the water gap sufficiently and other sources of water are needed. Hence, small-scale reservoirs may be supplemented with groundwater pumping. Sustainably doing so, however, is limited to the regions Casamance, Kédougou, and Tambacounda. These are regions which contain major rivers and receive above-average amounts of rainfall or have only limited agricultural activities and thus limited water demand - in short, regions with already favourable conditions. For semi-arid and arid regions, groundwater pumping can help to close the water gap too, but then likely in an unsustainable manner, that is, by (ever) lowering the groundwater head. Likely, a healthy holistic mix of measures is required to be able to improve water availability in Senegal, ranging from pumps via small-scale reservoirs to larger infrastructure projects such as dams. Which mix is most effective will have to be assessed per region individually.

It is important to note that these results should not be taken at face value. While the approach taken was thoroughly devised and all evaluation and benchmark metrics were satisfying, some aspects of the reservoir design approach may need improvement. After all, it must be kept in mind that the here presented approach is a first attempt to implement small-scale reservoirs into a large-scale hydrological model.

For instance, one limitation of the method used for selecting reservoirs using a selection area is that it allows for the selection of reservoirs in adjacent cells but within different selection areas. In that case, the downstream reservoir may receive insufficient inflows because of water retention by the upstream reservoir. Hence, a minimum distance between two reservoirs should be imposed. Besides, in the current parameterization, reservoirs can be overexploited in areas with much agricultural land, that is they are too small for the area they are ought to irrigate, and the supply of irrigation water from reservoirs to cropland cells within the respective abstraction zone is therefore minimal. Decreasing the size of the abstraction zone would remove cells farther away from the river from irrigation water supply, but it could potentially improve reservoir performance in areas where cropland density is high along the river. The size of the abstraction zones should additionally account for irrigation water need for multiple crops and not one dominant one as done here, and probably be a function of reservoir dimensions too. Moreover, the way evaporation losses are treated to determine the actual reservoir volume may need to be revisited. Last, the – with respect to the reservoirs – relatively simple schematization of the groundwater pumping should be advanced, for example by calibrating MODFLOW parameters with local data.

The agricultural water gap is not solely a function of water availability, but also of crop water demand. Hence, the here used crop coefficient approach does not account for nutrient limitations. As such, the water gap may be smaller than simulated here since the low nutrient input in Senegal results in only 20 % of water-limited yields due to lower plant transpiration in low-input systems (Van Ittersum et al., 2016). This means that less water than assumed is needed to fulfil the water demand of the achievable crop yield. In turn, this means that small-scale reservoirs and groundwater pumping may be able to close the water gap to a greater extent than simulated here. To capture this important interplay, future studies should therefore combine hydrologic simulations with more advanced crop growth models where different nutrient intensification strategies can be simulated.

Despite this first approach to implement small-scale reservoirs into a large-scale model leaving room for improvement, some general remarks can be made. For one, the lack of precipitation now and even more so in the future is a serious threat for food production in Senegal. While lower rainfall amounts and shorter rainy seasons may force farmers who want to intensify their cropping systems to move from rain-fed to irrigated agriculture, our results indicate that maintaining the same level of agricultural productivity will be challenging. Particularly the drier North will need additional attention for a socially-just transition. As our results suggest, the combined effect of small-scale reservoirs and groundwater pumping can be a viable option in some regions, while considerations about unsustainable groundwater use are in place for others. Moreover, the approach taken here is very general in that it does not consider local characteristics but aims to define a global set of rules to design small-scale measures across all regions. Devising suitable locations and dimensions of reservoirs does, however, require a bespoke approach per region and not a "one size fits all" approach as tested here. To that end, the hydrological model needs to reflect this spatial variability. Moreover, collaboration with local experts is paramount in more detailed studies to advance the here presented promising blueprint.

In this study, we merely looked at the hydrological potential of small-scale reservoirs and pumping at the local to regional scale. At the country scale, however, other considerations than those made here may be valid. For instance, it may be that small-scale reservoirs have positive impacts at the local scale, but that, compared to a few large reservoirs, the accumulated impact of many small-scale reservoirs on country-scale water management may be negative due to too much water or sediment retention. How to balance both sides should be subject of future research.

What we also did not consider is the economic feasibility. Hence, the costs of constructing small-scale reservoirs and equipping farmers with pumps to meet their water demand need to be contrasted against their (monetary) benefit. Additionally, other physical processes such as salinisation and its effects on soil productivity are not accounted for. By doing so, the hydrological potential of small-scale reservoirs and groundwater pumping can be severely reduced, especially in coastal regions.

Despite the first-order approach used and the uncertainty of our results, this study shows that there is an imminent need to devise measures for a just climate transition. Considering expected rainfall reduction and continued nutrient limitation of crops, it is detrimental to enable farmers to remain producing food for self-sufficiency and trade. The generated income may be used for

education, farm investments, and healthcare to alleviate poverty (Giordano et al., 2012; Hussain and Hanjra, 2004); in short, to build and improve resilience against climate change. With the here proposed blueprint, follow-up studies have a starting point to work out the hydrological requirements of small-scale measures in more detail. At the current stage, however, the here presented results and conclusions should not be used for actual decision-making but rather as a first analysis that provides a first step towards showing how hyper-resolution global-scale hydrological modes can be "locally relevant" (Bierkens et al., 2015).

Author statement

All named authors declare that they are knowledgeable about their authorship on this revised document.

CRediT authorship contribution statement

Jannis M. Hoch: Writing – original draft, Visualization, Supervision, Software, Methodology, Investigation, Formal analysis, Data curation, Conceptualization. **Anna C. Hoogeveen:** Writing – review & editing, Validation, Software, Methodology, Formal analysis, Data curation. **Edwin H. Sutanudjaja:** Writing – review & editing, Validation, Investigation, Data curation. **L.P.H. (Rens) van Beek:** Writing – review & editing, Software, Methodology, Data curation, Conceptualization. **Niko Wanders:** Writing – review & editing, Supervision, Software, Methodology, Investigation, Formal analysis, Data curation, Conceptualization. **Marc F.P. Bierkens:** Writing – review & editing, Supervision, Methodology, Funding acquisition, Conceptualization.

Declaration of Competing Interest

The authors declare that they have no known competing financial interests or personal relationships that could have appeared to influence the work reported in this paper.

Acknowledgements

JMH, EHS, and MPFB acknowledge funding by Climate-KIC under the ARISE project. Parts of the simulations were performed on the Dutch supercomputer Snellius provided by SURF.

Appendix A. Model set-up

A1 Meteorological input

W5E5 v2.0 precipitation data was downscaled to 150 arc-seconds with CHIRPS data, whereas ERA5-Land data was downloaded at this spatial resolution. Despite careful execution, Fig. 14 shows still some artefacts from the underlying coarser resolution. While they do not affect the outcome of the study, further work should aim at improved downscaling methods. To eventually derive at the 30 arc-seconds spatial resolution at which the model was run, the meteorological input data was resampled. Please see the supporting material in Hoch et al. (2023) for a detailed description.

PCR calculates actual evaporation based on land-cover-specific potential evaporation, calculated using the Penman-Monteith method. The input variables for this method, including reference potential evaporation, net radiation, wind speed, and vapor pressure deficit, were obtained from the ERA5-Land dataset (Muñoz-Sabater et al., 2021), along with the crop coefficient.

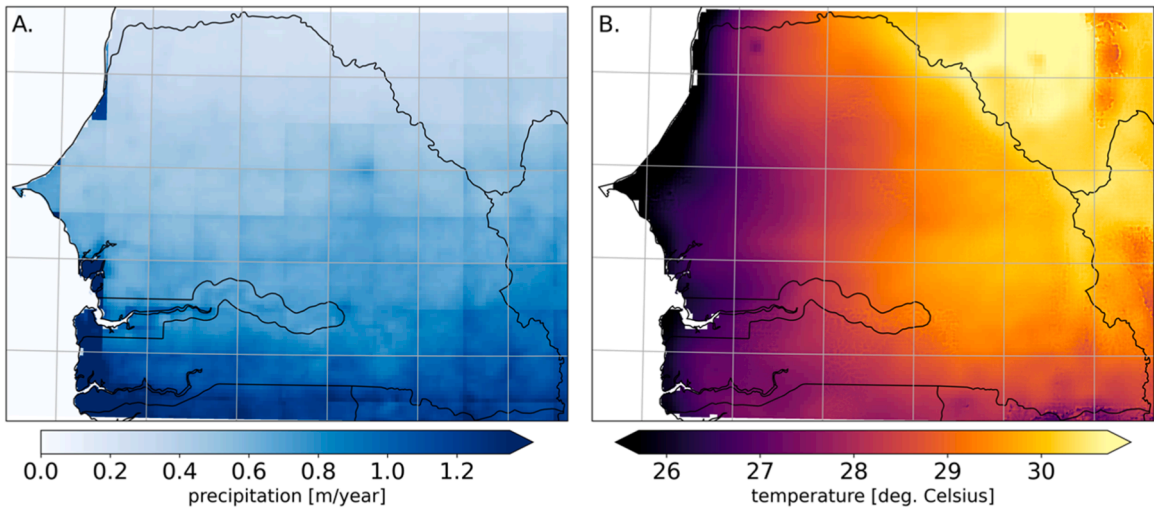


Fig. 14. A.) Average annual precipitation as used as input to PCR-GLOBWB over Senegal; B) Idem, but then average monthly temperature.

A2 Land cover

First, the cropland and natural vegetation areas were derived from Xiong et al. (2017). The cropland was then combined with a crop map from EOSTAT (2018), yielding the crop map shown in Fig. 2. It was assumed that all crops, except for irrigated rice, have one growing season per year with no crop rotation. The simulated growing season starts in June and ends in September for millet and sorghum (Allen et al., 1998; Araya et al., 2022), or ends in October for groundnuts, maize, cowpeas, and flooded rice (Allen et al., 1998; Djaman et al., 2019; Faye et al., 2020; Mady et al., 2020). Irrigated rice was assumed to have two growing seasons: the first from March to June, followed immediately by the second from July to October (Allen et al., 1998; Djaman et al., 2019; Faye et al., 2020).

Then, new values for the crop coefficient were obtained from the literature and assigned to the different crop types. These values vary based on the development stage of each crop, which was assumed to change monthly. The crop coefficient cycle for irrigated rice remained the same throughout both growing seasons. Furthermore, PCR requires information on the maximum rooting depth of crops and the fraction of roots in the first and second soil column. New values were introduced for all non-paddy crops (groundnuts, maize, millet, cowpeas, and sorghum). These values were assumed to remain constant over time.

A3 Reservoir design and implementation

Fig. 15 shows a flow chart of the process leading to the identification of suitable reservoir locations and sizes.

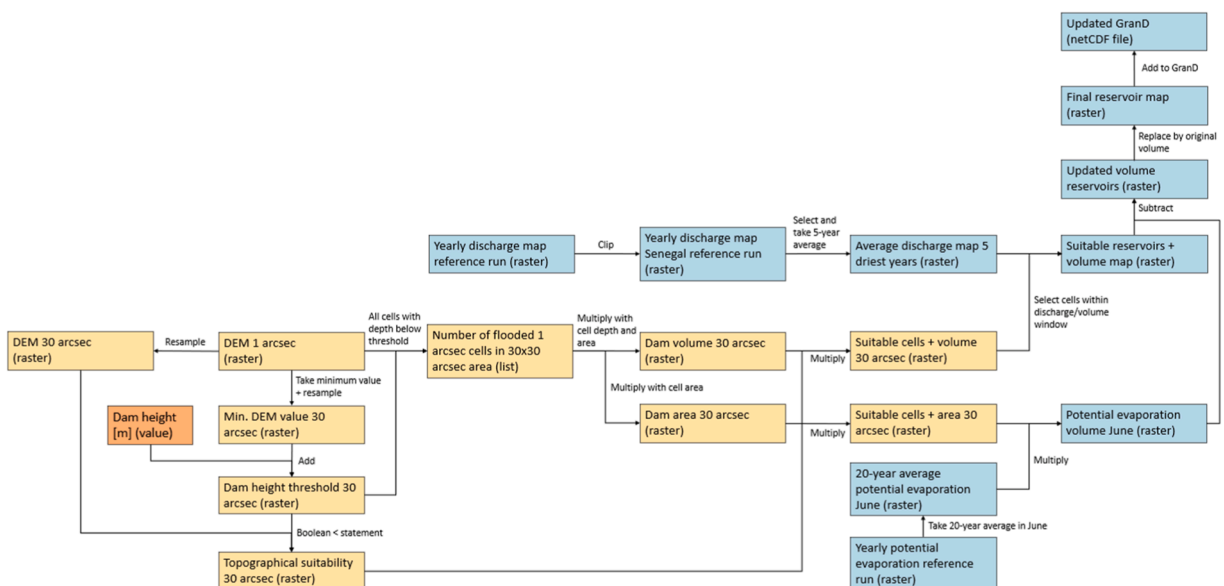


Fig. 15. Flow chart how the size and locations of suitable small-scale reservoirs are derived using a hydrological and topographical analysis.

A4 Hydrological analysis

From the GranD database (Lehner et al., 2011), a relationship between reservoir inflow and reservoir volume was derived first (Fig. 16). Hereby, we excluded both the lowest 25th percentile of reservoir volume as inflow into the smallest reservoirs may be overestimated by the coarse spatial resolution (12 km) of the runoff estimates used for parts of the dataset. Similarly, we excluded reservoirs exceeding the 75th percentile of reservoir volume to exclude the World's largest reservoirs such as the Three Gorges Dam in China, which are not representative for our study. Furthermore, we excluded reservoirs with a modeled negligible or intermittent inflow as they either could run dry due to the high evaporation rates in the Sahel (Mady et al., 2020) and because reservoirs made from earth materials may not be resistant to the expected flashy runoff behavior.

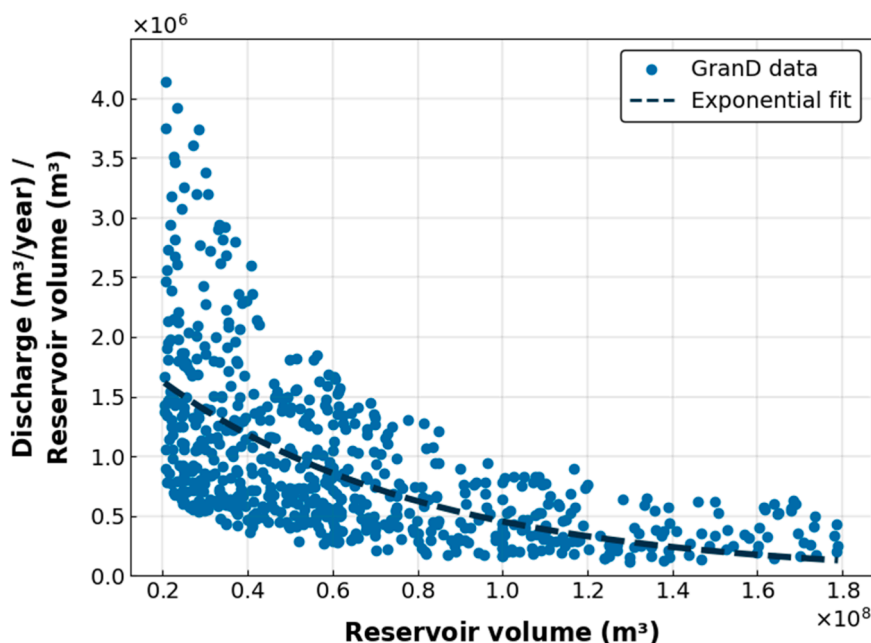


Fig. 16. Relation between discharge into a reservoir divided by reservoir volume versus reservoir volume. The dots are adapted from the GranD database, the line presents the exponential fit of the data.

Appendix B. Results and discussion

B1 Reference water gap

The influence of precipitation on the water gap becomes evident by comparing the regions of Thiès and Kaolack. Although Thiès has fewer cropland cells than Kaolack, it has a higher total water gap. The water gap per cell in Kaolack is $1.02 \times 10^5 \text{ m}^3$ where total annual precipitation is 646 mm (Fig. 16), compared to $1.45 \times 10^5 \text{ m}^3$ in Thiès (Table 3), with a total annual precipitation of 573 mm. The effect of precipitation on the water gap is particularly noticeable in Saint-Louis, which has the second highest water gap. With an annual precipitation of 288 mm, the water gap is $1.6 \times 10^9 \text{ m}^3$, while the number of cropland cells is only 1868. Nevertheless, it should be noted that agriculture in Saint-Louis was mainly developed as irrigated agriculture, with crops that utilise water from the Senegal River.

In the current model set-up, the size of the abstraction zones (Section 3.2.3) has been reduced to 2×2 cells. This entails that irrigation schemes can reach a maximum distance of 1273 m, while an extensive network of irrigation channels exist, with irrigation channels of up to 70 km long (Bouisse et al., 2011). Therefore, the water gap in Saint-Louis is likely overestimated, since these irrigation channels are not implemented into the model.

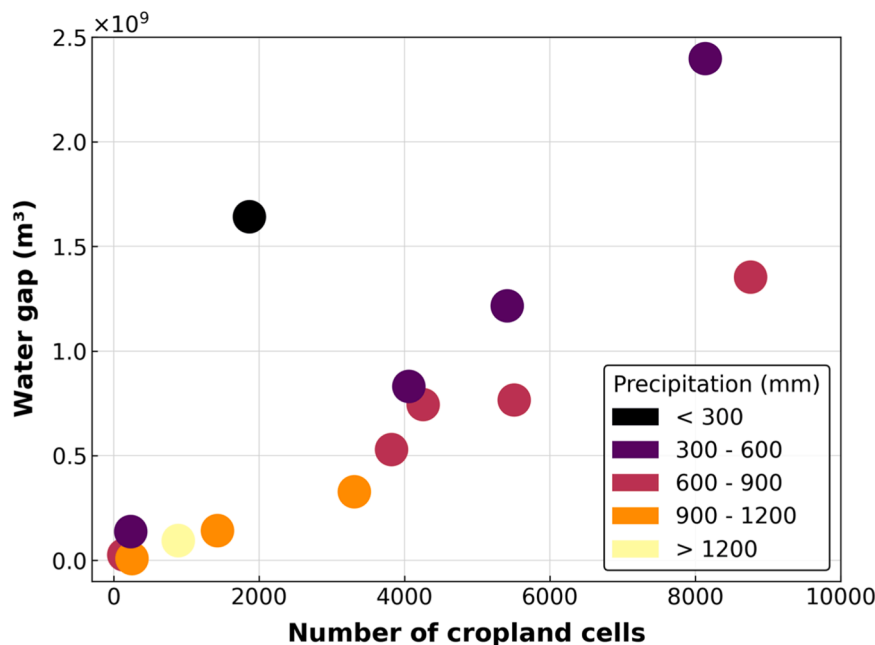


Fig. 17. Total yearly water gap (m^3) in the reference simulation versus the number of cropland cells, plotted for the fourteen regions in Senegal. The color of the markers presents the total yearly precipitation, averaged over the period 2000–2019.

Table 4

The total yearly water gap (m^3) per region in Senegal, averaged over the period 2000–2019, in the reference simulation. Columns B3.5–B5.10 show the decrease in water gap (%) after the implementation of reservoirs in the B simulations.

Region	Reference	B3.5	B4.5	B5.5	B3.10	B4.10	B5.10
Dakar	2.66×10^7	3.86	0.12	0.13	0.10	0.12	0.13
Diourbel	1.22×10^9	0.03	0.08	0.01	0.02	0.01	0.01
Fatick	7.44×10^8	0.37	0.27	0.13	0.18	0.10	0.11
Kédougou	8.57×10^6	2.04	6.27	4.09	2.04	4.38	2.85
Kaffrine	1.35×10^9	0.33	0.39	0.12	0.12	0.24	0.06
Kaolack	7.66×10^8	0.54	0.56	0.16	0.23	0.29	0.13
Kolda	3.27×10^8	2.70	3.89	3.04	1.26	1.49	0.98
Louga	2.40×10^9	0.01	0.01	0.00	0.01	0.00	0.00
Matam	1.37×10^8	0.00	0.00	0.00	0.00	0.00	0.00
Sédhiou	1.42×10^8	2.51	4.89	3.79	1.08	2.03	1.54
Saint-Louis	1.64×10^9	0.00	0.00	0.00	0.01	0.00	0.00
Tambacounda	5.29×10^8	0.64	0.68	0.19	0.32	0.36	0.16
Thiès	8.31×10^8	0.07	0.04	0.05	0.05	0.03	0.03
Ziguinchor	9.43×10^7	1.64	3.67	4.92	1.06	1.39	2.47
Total	1.02×10^{10}	0.30	0.39	0.25	0.14	0.18	0.12

B2 Reservoir simulations

Fig. 18 illustrates the cropland distribution in Senegal, along with the regions and the reservoirs implemented in simulation B4.5. Table 4 provides values per region for the number of cropland cells, water gap per cropland cell and total water gap (Fig. 8), number of reservoirs, number of cropland cells per reservoir, and the decrease in water gap after the implementation of reservoirs in simulation B4.5.

First of all, Fig. 9 showed that the decrease in water gap in the Kaolack and Kaffrine regions was 0–1 %. However, these regions have a relatively high number of reservoirs, with 150 and 80 respectively. The negligible decrease in water gap at the regional level may be caused by the large number of cropland cells compared to the number of reservoirs. Table 4 demonstrates that regions with a low number of cropland cells per reservoir exhibit a higher decrease in water gap. For example, Kédougou, Ziguinchor, Sédhio, and Kolda have between 13 and 21 cropland cells per reservoir, resulting in a decrease in water gap of 3.67–6.27 %. In contrast, Kaolack and Kaffrine have 69 and 58 cropland cells per reservoir respectively, leading to a decrease in water gap of only 0.56 % and 0.39 %. Similarly, Thiès, Fatick, Diourbel, and Louga show minimal decreases in water gap, which may be attributed to a high number of cropland cells per reservoir.

Moreover, Saint-Louis and Matam have no reservoirs implemented, as the discharge in these regions (Fig. 3) is insufficient to meet the hydrological requirements. Furthermore, Tambacounda has 39 cropland cells per reservoir, but a decrease in water gap of only 0.21 %. This discrepancy between the number of cropland cells and reduction in water gap might be due to the dispersion of cropland

cells. If a reservoir is located on a cropland cell but is surrounded by non-cropland cells, it cannot be used for irrigation and as a result, irrigation water from the reservoirs cannot effectively reduce the water gap.

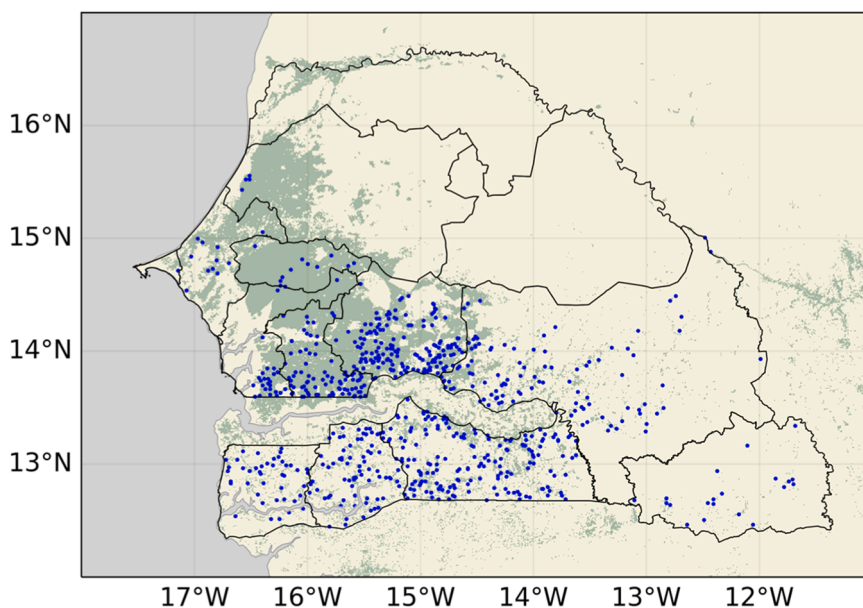


Fig. 18. Location of reservoirs implemented in simulation B4.5 (blue dots) and the cropland (green) (Xiong et al., 2017). The black lines mark the fourteen regions of Senegal (Hijmans, 2015).

Table 5

Number of cropland cells, water gap per cropland cell (m^3) (reference simulation), total water gap (m^3) (reference simulation), number of reservoirs, number of cropland cells divided by the number of reservoirs, and the decrease in water gap after the implementation of reservoirs in simulation B4.5, for every region in Senegal, averaged over the period 2000–2019.

Region	Cropland (cells)	Per cell $\times 10^5$	Total $\times 10^7$	Reservoirs	Cropland/ reservoir	Decrease (%)
Kédougou	253	0.26	0.9	20	13	6.27
Dakar	140	2.17	2.7	1	140	0.12
Ziguinchor	889	1.25	9.4	43	21	3.67
Matam	236	4.94	13.7	0	0	0.00
Sédhiou	1428	1.11	14.2	73	20	4.89
Kolda	3311	0.76	32.7	167	20	3.89
Tambacounda	3822	1.43	52.9	99	39	0.68
Fatick	4257	1.53	74.4	28	152	0.27
Kaolack	5510	1.02	76.6	80	69	0.56
Thiès	4060	2.45	83.1	11	369	0.04
Diourbel	5414	2.23	121.6	11	492	0.08
Kaffrine	8761	1.36	135.3	150	58	0.39
Saint-Louis	1868	8.36	164.2	0	0	0.00
Louga	8136	3.26	239.7	4	2034	0.01

Data availability

Data will be made available on request.

References

- Acheampong, D., Balana, B.B., Nimoh, F., Abaidoo, R.C., 2018. Assessing the effectiveness and impact of agricultural water management interventions: the case of small reservoirs in northern Ghana. *Agric. Water Manag.* 209, 163–170. <https://doi.org/10.1016/j.agwat.2018.07.009>.
- Affholder, F., Poeydebat, C., Corbeels, M., Scopel, E., Tittonell, P., 2013. The yield gap of major food crops in family agriculture in the tropics: assessment and analysis through field surveys and modelling. *Field Crops Res.* 143, 106–118.
- Allen, R.G., Pereira, L.S., Raes, D., Smith, M., 1998. Crop evaporation–guidelines for computing crop water requirements–FAO Irrigation and drainage paper 56. Food Agric. Organ. U. N. Rome 300.
- Altchenko, Y., Villholth, K.G., 2015. Mapping irrigation potential from renewable groundwater in Africa – a quantitative hydrological approach. *Hydrol. Earth Syst. Sci.* 19, 1055–1067. <https://doi.org/10.5194/hess-19-1055-2015>.

- ANACIM, WFP Office for Climate Change, Environment and Disaster Risk Reduction, WFP Food Security Analysis Service, Columbia University International Research Institute for Climate and Society (IRI), and WFP Country Office in Senegal: Climate risk and food security in Senegal: Analysis of climate impacts on food security and livelihoods, World Food Programme, 2014.
- Anon: WFDE5 over land merged with ERA5 over the ocean (W5E5 v2.0), <https://doi.org/10.48364/ISIMIP.342217>, 2021.
- Araya, A., Jha, P.K., Zambreski, Z., Faye, A., Ciampitti, I.A., Min, D., Gowda, P.H., Singh, U., Prasad, P.V.V., 2022. Evaluating crop management options for sorghum, pearl millet and peanut to minimize risk under the projected midcentury climate scenario for different locations in Senegal. *Clim. Risk Manag.* 36, 100436. <https://doi.org/10.1016/j.crm.2022.100436>.
- Bense, V.F., Gleeson, T., Loveless, S.E., Bour, O., Scibek, J., 2013. Fault zone hydrogeology. *Earth-Sci. Rev.* 127, 171–192. <https://doi.org/10.1016/j.earscirev.2013.09.008>.
- Bernards, N., 2021. Latent surplus populations and colonial histories of drought, groundnuts, and finance in Senegal. *Geoforum* 126, 441–450.
- Bierkens, M.F.P., Wada, Y., 2019. Non-renewable groundwater use and groundwater depletion: a review. *Environ. Res. Lett.* 14, 063002. <https://doi.org/10.1088/1748-9326/ab1a5f>.
- Bierkens, M.F.P., Bell, V.A., Burek, P., Chaney, N., Condon, L.E., David, C.H., de Roo, A., Döll, P., Drost, N., Famiglietti, J.S., Flörke, M., Gochis, D.J., Houser, P., Hut, R., Keune, J., Kollet, S., Maxwell, R.M., Reager, J.T., Samaniego, L., Sudicky, E., Sutanudjaja, E.H., van de Giesen, N., Winsemius, H., Wood, E.F., 2015. Hyper-resolution global hydrological modelling: what is next?: “Everywhere and locally relevant.” *Hydrol. Process.* 29, 310–320. <https://doi.org/10.1002/hyp.10391>.
- Bouisse, T., Baume, J.-P., Gassama, M., 2011. The use of hydraulic models to optimize the rehabilitation of an open channel irrigation system: the example of the senegal river delta irrigation system. *Irrig. Drain.* 60, 308–317. <https://doi.org/10.1002/ird.581>.
- Brandt, M.J., Johnson, K.M., Elphinston, A.J., Ratnayaka, D.D., 2017. Dams and reservoirs. In: *Twort's Water Supply*. Elsevier, pp. 159–204. <https://doi.org/10.1016/B978-0-08-100025-0.00005-3>.
- de Bruin, S. de, Hoch, J., Bruijn, J. de, Hermans, K., Maharjan, A., Kumm, M., Vliet, J. van, 2024. Scenario projections of South Asian migration patterns amidst environmental and socioeconomic change. *Glob. Environ. Change* 88, 102920. <https://doi.org/10.1016/j.gloenvcha.2024.102920>.
- Brunner, M.I., Slater, L., Tallaksen, L.M., Clark, M., 2021. Challenges in modeling and predicting floods and droughts: a review, *WIREs. Water* 8. <https://doi.org/10.1002/wat2.1520>.
- Cecchi, P., Meunier-Nikiema, A., Moiroux, N., Sanou, B.: Towards an Atlas of Lakes and Reservoirs in Burkina Faso, 2009.
- CIAT, BFS/USAID, 2016. *Climate-Smart Agriculture in Senegal. CSA Country Profiles for Africa Series, International Center for Tropical Agriculture (CIAT); Bureau for Food Security. United States Agency for International Development (BFS/USAID), Washington, D.C.*
- Cobbing, J., Hiller, B., 2019. Waking a sleeping giant: realizing the potential of groundwater in Sub-Saharan Africa. *World Dev.* 122, 597–613. <https://doi.org/10.1016/j.worlddev.2019.06.024>.
- Comité de Pilotage du Livre Bleu Sénégal: Livre bleu / Rapport pays: Sénégal, 2009.
- D'Alessandro, S., Abdoulaye Fall, A., Grey, G., Simpkin, S., Wane, A., 2015. *Senegal agricultural sector risk assessment. Agric. Glob. Pract. Tech. Assist. Pap.*
- Degeorges, A., Reilly, B.K., 2006. Dams and large scale irrigation on the Senegal River: impacts on man and the environment. *Int. J. Environ. Stud.* 63, 633–644. <https://doi.org/10.1080/00207230600963296>.
- Djaman, K., Rudnick, D.R., Moukoubi, Y.D., Sow, A., Irmak, S., 2019. Actual evapotranspiration and crop coefficients of irrigated lowland rice (*Oryza sativa* L.) under semi-arid climate. *Ital. J. Agron.* 14, 19–25. <https://doi.org/10.4081/ija.2019.1059>.
- Doorenbos, J., Kassam, A., 1979. *Yield response to water*. FAO, Rome.
- Dorigo, W., Wagner, W., Albergel, C., Albrecht, F., Balsamo, G., Brocca, L., Chung, D., Ertl, M., Forkel, M., Gruber, A., Haas, E., Hamer, P.D., Hirschi, M., Ikonen, J., de Jeu, R., Kidd, R., Lahoz, W., Liu, Y.Y., Miralles, D., Mistelbauer, T., Nicolai-Shaw, N., Parinussa, R., Pratola, C., Reimer, C., van der Schalie, R., Seneviratne, S.I., Smolander, T., Lecomte, P., 2017. ESA CCI soil moisture for improved earth system understanding: state-of-the-art and future directions. *Remote Sens. Environ.* 203, 185–215. <https://doi.org/10.1016/j.rse.2017.07.001>.
- EOSTAT: Crop Mask (Senegal - 10m - 2018) - EOSTAT [Data set], 2018.
- Escobar, N., Bautista, I., Peña, N., Fenollosa, M.L., Osca, J.M., Sanjuán, N., 2022. Life cycle thinking for the environmental and financial assessment of rice management systems in the Senegal River Valley. *J. Environ. Manag.* 310, 114722. <https://doi.org/10.1016/j.jenvman.2022.114722>.
- Falconner, G.N., Corbeels, M., Boote, K.J., Affholder, F., Adam, M., MacCarthy, D.S., Ruane, A.C., Nendel, C., Whitbread, A.M., Justes, É., Ahuja, L.R., Akinseye, F.M., Alou, I.N., Amouzou, K.A., Anapalli, S.S., Baron, C., Basso, B., Baudron, F., Bertuzzi, P., Challinor, A.J., Chen, Y., Deryng, D., Elsayed, M.L., Faye, B., Gaiser, T., Galdos, M., Gaylor, S., Gerardeaux, E., Giner, M., Grant, B., Hoogenboom, G., Ibrahim, E.S., Kamali, B., Kersebaum, K.C., Kim, S., Laan, M., Leroux, L., Lizaso, J.I., Maestrini, B., Meier, E.A., Mequanint, F., Ndoli, A., Porter, C.H., Priesack, E., Ripoche, D., Sida, T.S., Singh, U., Smith, W.N., Srivastava, A., Sinha, S., Tao, F., Thornburn, P.J., Timlin, D., Traore, B., Twine, T., Webber, H., 2020. Modelling climate change impacts on maize yields under low nitrogen input conditions in sub-Saharan Africa. *Glob. Change Biol.* 26, 5942–5964. <https://doi.org/10.1111/gcb.15261>.
- Faye, A., Msangi, S., 2018. *Rainfall variability and groundwater availability for irrigation in Sub-Saharan Africa: evidence from the Niayes region of Senegal*. University Library of Munich, Germany.
- Faye, B., Sultan, B., Affholder, F., Gérard, F.: Impact of climate sensitivity on agriculture systems in West Africa: Case of Senegal, 2020.
- Felfelani, F., Lawrence, D.M., Pokhrel, Y., 2021. Representing Interwell Lateral Groundwater Flow and Aquifer Pumping in the Community Land Model. *Water Resour. Res.* 57. <https://doi.org/10.1029/2020WR027531>.
- Finger, D., Teodoru, C.: Case study Senegal River, Zürich, 2003..
- de Fraiture, C., Kouali, G.N., Sally, H., Kabre, P., 2014. Pirates or pioneers? Unplanned irrigation around small reservoirs in Burkina Faso. *Agric. Water Manag.* 131, 212–220. <https://doi.org/10.1016/j.agwat.2013.07.001>.
- Funk, C.C., Peterson, P.J., Landsfeld, M.F., Pedreros, D.H., Verdin, J.P., Rowland, J.D., Romero, B.E., Husak, G.J., Michaelson, J.C., Verdin, A.P.: A quasi-global precipitation time series for drought monitoring: U.S. Geological Survey Data Series 832, 4 p., U.S. Geological Survey, 2014., and <https://dxdoi.org/10.3133/ds832>, <https://dx.doi.org/10.3133/ds832>.
- GFDRR, 2011. *Climate Risk and Adaptation Country Profile: Senegal*. The World Bank.
- Giordano, M., de Fraiture, C., Weight, E., van der Blik, J., 2012. *Water for wealth and food security: supporting farmer-driven investments in agricultural water management. Synthesis report of the AgWater Solutions Project, IWMI*.
- de Graaf, I.E.M., Gleeson, T., (Rens) van Beek, L.P.H., Sutanudjaja, E.H., Bierkens, M.F.P., 2019. Environmental flow limits to global groundwater pumping. *Nature* 574, 90–94. <https://doi.org/10.1038/s41586-019-1594-4>.
- Gruber, A., Scanlon, T., van der Schalie, R., Wagner, W., Dorigo, W., 2019. Evolution of the ESA CCI Soil Moisture climate data records and their underlying merging methodology. *Earth Syst. Sci. Data* 11, 717–739. <https://doi.org/10.5194/essd-11-717-2019>.
- Gupta, H.V., Kling, H., Yilmaz, K.K., Martinez, G.F., 2009. Decomposition of the mean squared error and NSE performance criteria: implications for improving hydrological modelling. *J. Hydrol.* 377, 80–91. <https://doi.org/10.1016/j.jhydrol.2009.08.003>.
- Gutiérrez, J.M., Jones, R.G., Narisma, G.T., Muniz Alves, L., Amjad, M., Gorodetskaya, I.V., Grose, M., Klutse, N.A.B., Krakovska, S., Li, J., Martínez-Castro, D., Mearns, L.O., Mernild, S.H., Ngo-Duc, T., van den Hurk, B., Yoon, J.-H., 2021. Atlas. In: Masson-Delmotte, V., Zhai, P., Pirani, A., Connors, S.L., Péan, C., Berger, S., Caud, N., Chen, Y., Goldfarb, L., Gomis, M.I., Huang, M., Leitzell, K., Lonnoy, E., Matthews, J.B.R., Maycock, T.K., Waterfield, T., Yelekçi, Ö., Yu, R., Zhou, B. (Eds.), *Climate Change 2021: The Physical Science Basis. Contribution of Working Group I to the Sixth Assessment Report of the Intergovernmental Panel on Climate Change*. Cambridge University Press, Cambridge, United Kingdom and New York, NY, USA, Cambridge, United Kingdom and New York, NY, USA, pp. 1927–2058. <https://doi.org/10.1017/9781009157896.001>.
- Hawker, L., Uhe, P., Paulo, L., Sosa, J., Savage, J., Sampson, C., Neal, J., 2022. A 30 m global map of elevation with forests and buildings removed. *Environ. Res. Lett.* 17, 024016. <https://doi.org/10.1088/1748-9326/ac4d4f>.
- Hijmans, R.: First-level Administrative Divisions, Senegal, 2015. UC Berkeley, Museum of Vertebrate Zoology., 2015.

- Hoch, J.M., Sutanudjaja, E.H., Wanders, N., van Beek, R.L.P.H., Bierkens, M.F.P., 2023. Hyper-resolution PCR-GLOBWB: opportunities and challenges from refining model spatial resolution to 1 km over the European continent. *Hydrol. Earth Syst. Sci.* 27, 1383–1401. <https://doi.org/10.5194/hess-27-1383-2023>.
- Hussain, I., Hanjra, M.A., 2004. Irrigation and poverty alleviation: review of the empirical evidence. *Irrig. Drain.* 53, 1–15. <https://doi.org/10.1002/ird.114>.
- IFPRI, 2013. West African agriculture and climate change A comprehensive analysis. International Food Policy Research Institute, Washington, DC. <https://doi.org/10.2499/9780896292048>.
- Ilboudo Nébié, E.K., Ba, D., Giannini, A., 2021. Food security and climate shocks in Senegal: Who and where are the most vulnerable households? *Glob. Food Secur.* 29, 100513. <https://doi.org/10.1016/j.gfs.2021.100513>.
- ISCGM/DTGC: Rivers, Senegal., 2012.
- van Jaarsveld, B., Wanders, N., Sutanudjaja, E.H., Hoch, J., Droppers, B., Janzing, J., van Beek, R.L.P.H., Bierkens, M.F.P., 2024. A first attempt to model global hydrology at hyper-resolution. *EGUosphere* 1–32. <https://doi.org/10.5194/eguosphere-2024-1025>, 2024.
- Jayne, T.S., Mason, N.M., Burke, W.J., Ariga, J., 2018. Taking stock of Africa's second-generation agricultural input subsidy programs. *Food Policy* 75, 1–14.
- Knoben, W.J., Freer, J.E., Woods, R.A., 2019. Inherent benchmark or not? Comparing Nash–Sutcliffe and Kling–Gupta efficiency scores. *Hydrol. Earth Syst. Sci.* 23, 4323–4331. <https://doi.org/10.5194/hess-23-4323-2019>.
- Kumi, N., Abiodun, B.J., 2018. Potential impacts of 1.5^{°C} and 2^{°C} global warming on rainfall onset, cessation and length of rainy season in West Africa. *Environ. Res. Lett.* 13, 055009. <https://doi.org/10.1088/1748-9326/aab89e>.
- Lamat, J.P., Albergel, J., Bouchez, J.M., Descroix, L.: Monographie Hydrologique du Fleuve Gambie, Institut Français de Recherche Scientifique pour le Développement en Coopération, L'Organisation pour la mise en Valeur du Fleuve Gambie, 1990.
- Laube, W., Awo, M., Schraven, B.: Erratic rains and erratic markets: environmental change, economic globalisation and the expansion of shallow groundwater irrigation in West Africa, University of Bonn, Center for Development Research (ZEF), Bonn, 2008.
- Lehner, B., Liermann, C.R., Revenga, C., Vörösmarty, C., Fekete, B., Crouzet, P., Döll, P., Endejan, M., Frenken, K., Magome, J., Nilsson, C., Robertson, J.C., Rödel, R., Sinderof, N., Wissler, D., 2011. High-resolution mapping of the world's reservoirs and dams for sustainable river-flow management. *Front. Ecol. Environ.* 9, 494–502. <https://doi.org/10.1890/100125>.
- Leipert, F., Darmaun, M., Bernoux, M., Mphesha, M., 2020. The potential of agroecology to build climate-resilient livelihoods and food systems. FAO and Biovision, Rome.
- Lobell, D.B., Bänziger, M., Magorokosho, C., Vivek, B., 2011. Nonlinear heat effects on African maize as evidenced by historical yield trials. *Nat. Clim. Change* 1, 42–45. <https://doi.org/10.1038/nclimate1043>.
- Madione, D., Mall, I., Faye, S., Crane, E., Upton, K., Ó Dochartaigh, B., Bellwood-Howard, I., 2018. Africa groundwater atlas: hydrogeology of Senegal. *Br. Geol. Surv. Mady*, P., Lehmann, P., Gorelick, S.M., Or, D., 2020. Distribution of small seasonal reservoirs in semi-arid regions and associated evaporative losses. *Environ. Res. Commun.* 2, 061002. <https://doi.org/10.1088/2515-7620/ab92af>.
- Magatte, W., Tran Minh, D., Honoré, D.: Les ressources en eau, Bilan Rech. Agric. Agroaliment. Au Sénégal, 2005.
- Manikowski, S., Strapasson, A., 2016. Sustainability assessment of large irrigation dams in Senegal: a cost-benefit analysis for the Senegal River Valley. *Front. Environ. Sci.* 4. <https://doi.org/10.3389/fenvs.2016.00018>.
- Martens, B., Gonzalez Miralles, D., Lievens, H., Van Der Schalie, R., De Jeu, R.A., Fernández-Prieto, D., Beck, H.E., Dorigo, W., Verhoest, N., 2017. GLEAM v3: satellite-based land evaporation and root-zone soil moisture. *Geosci. Model Dev.* 10, 1903–1925. <https://doi.org/10.5194/gmd-10-1903-2017>.
- McClintock, N.C., Diop, A.M., 2005. Soil fertility management and compost use in Senegal's Peanut Basin. *Int. J. Agric. Sustain.* 3, 79–91. <https://doi.org/10.1080/14735903.2005.9684746>.
- McDonald, M., Harbaugh, A.: A modular three-dimensional finite-difference ground-water flow model: Techniques of WaterResources Investigations of the United States Geological Survey, Book 6, 1988.
- McSweeney, C., New, M., Lizzano, G., 2010. UNDP climate change country profiles: Senegal. U. Nations Dev. Program.
- Miralles, D.G., Holmes, T.R.H., De Jeu, R.A.M., Gash, J.H., Meesters, A.G.C.A., Dolman, A.J., 2011. Global land-surface evaporation estimated from satellite-based observations. *Hydrol. Earth Syst. Sci.* 15, 453–469. <https://doi.org/10.5194/hess-15-453-2011>.
- Muñoz-Sabater, J., Dutra, E., Agustí-Panareda, A., Albergel, C., Arduini, G., Balsamo, G., Boussetta, S., Choulla, M., Harrigan, S., Hersbach, H., Martens, B., Miralles, D.G., Piles, M., Rodríguez-Fernández, N.J., Soté, E., Buontempo, C., Thépaut, J.-N., 2021. ERA5-Land: a state-of-the-art global reanalysis dataset for land applications. *Earth Syst. Sci. Data* 13, 4349–4383. <https://doi.org/10.5194/essd-13-4349-2021>.
- Namara, R.E., Awuni, J., Barry, B., Giordano, M., Hope, L., Sarpong, E.O., Forkuor, G., 2011. Smallholder shallow groundwater irrigation development in the upper east region of Ghana. *International Water Management Institute (IWMI)*. <https://doi.org/10.5337/2011.214>.
- Onojeghwo, A.R., Balzter, H., Monks, P.S., 2017. Tropospheric NO₂ concentrations over West Africa are influenced by climate zone and soil moisture variability. *Atmos. Chem. Phys. Discuss.* <https://doi.org/10.5194/acp-2016-1128>.
- Owusu, S., Cofie, O., Mul, M., Barron, J., 2022. The significance of small reservoirs in sustaining agricultural landscapes in dry areas of West Africa: a review. *Water* 14, 1440. <https://doi.org/10.3390/w14091440>.
- Oya, C., Ba, C.O.: Les politiques agricoles 2000-2012: entre volontarisme et l'incohérence, in: Sénégal (2000-2012) Les institutions et politiques publiques à l'épreuve d'une gouvernance libérale., edited by: Diop, M. C., 149–178, 2013.
- Pavelic, P., Villhölth, K.G., Shu, Y., Rebelo, L.-M., Smakhtin, V., 2013. Smallholder groundwater irrigation in Sub-Saharan Africa: country-level estimates of development potential. *Water Int* 38, 392–407. <https://doi.org/10.1080/02508060.2013.819601>.
- Ranasinghe, R., Ruane, A.C., Vautard, R., Arnell, N., Coppola, E., Cruz, F.A., Dessai, S., Islam, A.S., Rahimi, M., Ruiz Carrascal, D., Sillmann, J., Sylla, M.B., Tebaldi, C., Wang, W., Zaaboul, R., 2021. Climate change information for regional impact and for risk assessment. In: Masson-Delmotte, V., Zhai, P., Pirani, A., Connors, S.L., Péan, C., Berger, S., Caud, N., Chen, Y., Goldfarb, L., Gomis, M.I., Huang, M., Leitzell, K., Lonnoy, E., Matthews, J.B.R., Maycock, T.K., Waterfield, T., Yelekçi, Ö., Yu, R., Zhou, B. (Eds.), *Climate Change 2021: The Physical Science Basis. Contribution of Working Group I to the Sixth Assessment Report of the Intergovernmental Panel on Climate Change*. Cambridge University Press, Cambridge, United Kingdom and New York, NY, USA, pp. 1767–1926. <https://doi.org/10.1017/9781009157896.001>.
- Ricome, A., Affholder, F., Gérard, F., Muller, B., Poeydebat, C., Quirion, P., Sall, M., 2017. Are subsidies to weather-index insurance the best use of public funds? A bio-economic farm model applied to the Senegalese groundnut basin. *Agric. Syst.* 156, 149–176. <https://doi.org/10.1016/j.agsy.2017.05.015>.
- Saruchera, D., Lautze, J., 2019. Small reservoirs in Africa: a review and synthesis to strengthen future investment. *International Water Management Institute (IWMI)*. <https://doi.org/10.5337/2019.209>.
- Senagosrosol: Évaluation environnementale stratégique des activités relatives à la promotion de l'irrigation dans les Niayes, le Bassin arachidier élargi à la région de Tambacounda et la Casamance, 2009.
- Siebert, S., Henrich, V., Frenken, K., Burke, J.: Global Map of Irrigation Areas version 5, 2013.
- Singer, M.B., Asfaw, D.T., Rosolem, R., Cuthbert, M.O., Miralles, D.G., MacLeod, D., Quichimbo, E.A., Michaelides, K., 2021. Hourly potential evapotranspiration at 0.1^{°C} resolution for the global land surface from 1981-present. *Sci. Data* 8, 224. <https://doi.org/10.1038/s41597-021-01003-9>.
- Sow, S., Nkonya, E., Meyer, S., Kato, E., 2016. Cost, drivers and action against land degradation in Senegal. In: Nkonya, E., Mirzabaev, A., Von Braun, J. (Eds.), *Economics of Land Degradation and Improvement – A Global Assessment for Sustainable Development*. Springer International Publishing, Cham, pp. 577–608. https://doi.org/10.1007/978-3-319-19168-3_19.
- Stephens, T., 2010. *Manual on small earth dams: a guide to siting, design and construction*. FAO, Rome.
- Sutanudjaja, E.H., Beek, R.L.P.H., van, Jong, S.M., de, Geer, F.C., van, Bierkens, M.F.P., 2011. Large-scale groundwater modeling using global datasets: a test case for the Rhine-Meuse basin. *Hydrol. Earth Syst. Sci.* 15, 2913–2935. <https://doi.org/10.5194/hess-15-2913-2011>.
- Sutanudjaja, E.H., van Beek, R., Wanders, N., Wada, Y., Bosmans, J.H.C., Drost, N., van der Ent, R.J., de Graaf, I.E.M., Hoch, J.M., de Jong, K., Karssenberg, D., López López, P., Peñenteiner, S., Schmitz, O., Straatsma, M.W., Vannamete, E., Wissler, D., Bierkens, M.F.P., 2018. PCR-GLOBWB 2: a 5 arcmin global hydrological and water resources model. *Geosci. Model Dev.* 11, 2429–2453. <https://doi.org/10.5194/gmd-11-2429-2018>.

- Thiam, S., Villamor, G.B., Kyei-Baffour, N., Matty, F., 2019. Soil salinity assessment and coping strategies in the coastal agricultural landscape in Djilor district, Senegal. *Land Use Policy* 88, 104191. <https://doi.org/10.1016/j.landusepol.2019.104191>.
- USAID, SWP: Senegal Water Resources Profile Overview, USAID, Sustainable Water Partnership, 2021.
- Van Ittersum, M.K., Van Bussel, L.G., Wolf, J., Grassini, P., Van Wart, J., Guilpart, N., Claessens, L., De Groot, H., Wiebe, K., Mason-D'Croz, D., et al., 2016. Can sub-Saharan Africa feed itself? *Proc. Natl. Acad. Sci.* 113, 14964–14969.
- Vanlauwe, B., Coyne, D., Gockowski, J., Hauser, S., Huising, J., Masso, C., Nziguheba, G., Schut, M., Van Asten, P., 2014. Sustainable intensification and the African smallholder farmer. *Curr. Opin. Environ. Sustain.* 8, 15–22. <https://doi.org/10.1016/j.cosust.2014.06.001>.
- Venot, J.-P., Hirvonen, M., 2013. Enduring controversy: small reservoirs in Sub-Saharan Africa. *Soc. Nat. Resour.* 26, 883–897. <https://doi.org/10.1080/08941920.2012.723306>.
- Verkaik, J., Sutanudjaja, E.H., Oude Essink, G.H.P., Lin, H.X., Bierkens, M.F.P., 2022. GLOBGM v1.0: a parallel implementation of a 30 arcsec PCR-GLOBWB-MODFLOW global-scale groundwater model. *Geosci. Model Dev. Discuss.* 1–27. <https://doi.org/10.5194/gmd-2022-226>.
- World Bank, World Development Indicators: Poverty headcount ratio at \$2.15 a day (2017 PPP) (% of population) - Senegal [Date file], 2018.
- World Bank, World Development Indicators: GDP (current US\$) - Senegal [Date file], 2021a.
- World Bank, World Development Indicators: Population, total - Senegal [Date file], 2021b.
- Xie, H., You, L., Wielgosz, B., Ringler, C., 2014. Estimating the potential for expanding smallholder irrigation in Sub-Saharan. *Afr., Agric. Water Manag.* 131, 183–193. <https://doi.org/10.1016/j.agwat.2013.08.011>.
- Xiong, J., Thenkabail, P., Tilton, J., Gumma, M., Teluguntla, P., Congalton, R., Yadav, K., Dungan, J., Oliphant, A., Poehnel, J., Smith, C., Massey, R.: NASA Making Earth System Data Records for Use in Research Environments (MEaSUREs) Global Food Security-support Analysis Data (GFSAD) Cropland Extent 2015 Africa 30 m V001 [Data set], 2017. <https://doi.org/10.5067/MEASURES/GFSAD/GFSAD30AFCE.001>.